Immature fruit abscission is triggered by hormonal changes in the seed coat of avocado

Amnon Haberman[1,2], Marc Goetz[1], Christine Böttcher[1], Philip Hands[3], Suzanne M. Maffei[1] and Harley M. Smith[1*]

[1]CSIRO Agriculture and Food, PO Box 200, Glenside, SA 5065, Australia

[2]Queensland Department of Primary Industries, Bundaberg Research Station, QLD, 4670, Australia

[3]CSIRO Agriculture and Food, GPO Box 1700, Canberra, ACT 2601, Australia

Running Title: Developmental regulation of avocado fruitlet abscission

*Author for correspondence: Harley M. Smith, Ph.D., Commonwealth Scientific and Industrial Research Organization (CSIRO), Agriculture & Food, PO Box 200, Glenside, South Australia, 5065, Australia. Tel: +61 882738131; email: harley.smith@csiro.au; ORCID ID: 0000-0003-1304-9973

Highlight statement: Results from this manuscript suggest that avocado fruitlet abscission is mediated by a hormone-driven transcriptome reprogramming that activates a senescence program of development in the seed coat to trigger abscission.

ACCEPTED MANUSCRIPT

© The Author(s) 2026. Published by Oxford University Press on behalf of Society for Experimental Biology. This is an Open Access article distributed under the terms of the Creative Commons Attribution-NonCommercial License (https://creativecommons.org/licenses/by-nc/4.0/), which permits non-commercial re-use, distribution, and reproduction in any medium, provided the original work is properly cited. For commercial re-use, please contact reprints@oup.com for reprints and translation rights for reprints. All other permissions can be obtained through our RightsLink service via the Permissions link on the article page on our site—for further information please contact journals.permissions@oup.com.

Downloaded from https://academic.oup.com/jxb/advance-article/doi/10.1093/jxb/erag289/8709372 by Qld Dept of Employment, Economic Development & Innovation user on 19 June 2026

Abstract

Avocado (*Persea americana* Mill.) is an economically important tree crop that exhibits a high rate of immature fruit abscission (IFA), reducing yield. As the seed coat derived from recently abscised fruitlets displays a senescence phenotype, we hypothesized that the seed coat plays a critical role in initiating IFA. Here, we show that fruitlets fated to abscise undergo growth arrest before shrinking and detaching from the tree. Comparative RNAseq analysis indicates that growth arrest is associated with a transcriptome reprogramming that is first initiated in the seed coat then transmitted to pericarp and embryo. Gene expression and hormone profiling results indicate that fruitlet growth arrest is associated with a decline in auxin activity and an increase in abscisic acid, the ethylene precursor, 1-aminocyclopropane-1-carboxylic acid, and the bioactive jasmonate, jasmonoyl-isoleucine, in the seed coat. At a late stage of growth arrest, transcriptomic signatures further suggest that a dormancy-like program of development is induced in the seed and a senescence phenotype is activated in the seed coat. Together, our data indicate that avocado IFA is initiated by hormone-driven transcriptome reprogramming that functions to transition the seed coat to a senescence program of development, which induces growth arrest, seed dormancy and ultimately, fruitlet abscission.

Keywords: Fruit abscission, seed coat, auxin, abscisic acid, ethylene, jasmonic acid, senescence, seed dormancy, *Persea americana*

Abbreviations: IFA, immature fruit abscission; **AZ**, abscission zone; **IAA**, indole-3-acetic acid; **IAA-Asp**, IAA-aspartate; **ABA**, PA, phaseic acid; **DPA**, dihydrophaseic acid; **ET**, ethylene; **ACC**, 1-aminocyclopropane-1-carboxylic acid; **JA**, jasmonic acid; **JA-Ile**, (+)-7-iso-jasmonoyl-L-isoleucine; **DAFB**, days after full bloom; **DEG**, differentially expressed gene; **NGA**, natural growth arrest, **DEGA**, defoliation early growth arrest; **DGA**, defoliation late growth arrest.

ACCEPTED MANUSCRIPT

Downloaded from https://academic.oup.com/jxb/advance-article/doi/10.1093/jxb/erag289/8709372 by Qld Dept of Employment, Economic Development & Innovation user on 19 June 2026

Introduction

Plant organs, including fruit, follow a highly regulated developmental sequence that begins with growth followed by maturation and culminates with senescence (Fenn and Giovannoni, 2021; Pautot *et al.*, 2025). The growth phase is characterized by active patterns of cell division and expansion. During maturation, cell differentiation is activated to establish specialized cells and tissues essential for organ function. As organs age, they undergo senescence, a programmed degenerative process frequently associated with abscission (Patharkar and Walker, 2019; Pautot *et al.*, 2025). In addition to age-related senescence, environmental stress, pathogen attack, or nutrient deficiency can also trigger a programmed degeneration process, often leading to the detachment of both mature and immature organs.

In many economically important fruit tree crops, a substantial proportion of immature fruit undergo abscission during the growth phase of development (Sawicki *et al.*, 2015; Sadka *et al.*, 2023). It is hypothesized that immature fruit abscission (IFA) results from feedback interactions between expanding vegetative shoots and developing fruit, as well as among fruitlets (Sawicki et al., 2015; Sadka et al., 2023). According to this model, vegetative shoots and fruitlets with greater growth potential induce abscission in fruitlets with a lower growth potential. In apple (*Malus domestica*), applying fruitlet thinning agents that likely enhance feedback interactions among developing fruitlets causes a large population of immature fruit to abscise (Botton and Ruperti, 2019). Further, after application of fruit thinning agents, experimental studies suggest that fruitlets fated to abscise undergo growth arrest prior to abscission (Ward and Marini, 1999; Greene *et al.*, 2013). Thus, it appears that the primary effect of these feedback interactions in fruitlets fated to abscise is to inhibit growth before abscission is activated in the pedicel.

In developing fruit, auxin is primarily produced in seeds, where it promotes growth and coordinates seed and fruit development (Kumar *et al.*, 2014; Figueiredo and Köhler, 2018; Fenn and Giovannoni, 2021). It is generally accepted that polar transport of auxin from the developing fruitlet through the pedicel suppresses the activation of the abscission zone (AZ) (Sawicki *et al.*, 2015; Pautot *et al.*, 2025). However, if the level of auxin is reduced in the AZ by a disruption in the polar auxin transport system, cell separation can be activated by ethylene (ET) (Sawicki *et al.*, 2015; Pautot *et al.*, 2025). Consequently, intra-organ signaling events initiated within fruitlets fated to abscise are predicted to influence auxin production in the seed and/or its export through the pedicel, thereby permitting the activation of the AZ (Sawicki *et al.*, 2015; Botton and Ruperti, 2019).

ACCEPTED MANUSCRIPT

Downloaded from https://academic.oup.com/jxb/advance-article/doi/10.1093/jxb/erag289/8709372 by Qld Dept of Employment, Economic Development & Innovation user on 19 June 2026

Apple has served as model system for investigating intra-organ signaling events associated with IFA (Sawicki *et al.*, 2015; Botton and Ruperti, 2019). Studies indicate that apple fruitlet abscission is initiated in the cortex by increased production of ET and abscisic acid (ABA) (Botton *et al.*, 2011). ET is proposed to act as a mobile signal that diffuses from the cortex to the seed, where it induces seed abortion (Eccher et al., 2015). Seed abortion is thought to reduce auxin transport through the pedicel, thereby enabling ET to activate cell separation processes in the AZ (Sawicki *et al.*, 2015; Botton and Ruperti, 2019). The role of ABA is less clear as it has been speculated that ABA production in the cortex is due to a stress response and may not play a direct role in initiating embryo abortion (Botton and Ruperti, 2019). Although apple provides a valuable framework for understanding IFA, it remains unclear whether the signaling mechanism(s) that functions upstream of AZ activation is conserved across different fruit tree species.

Avocado (*Persea americana* Mill.) exhibits a high rate of IFA starting in spring within two weeks after flowering, which continues through the summer before declining in autumn (Salazar-Garcia *et al.*, 2013). A substantial proportion of fruitlets that abscise during the first 2-3 weeks after flowering are unfertilized, whereas those that abscise after approximately four weeks are typically fertilized (Sedgley, 1980; Garner and Lovatt, 2016). Notably, fruitlets that drop during summer that exceed 20 mm in diameter display a premature senescence phenotype in the seed coat (Garner and Lovatt, 2016). Experimental observations show that weakly attached fruitlets that were likely in the final stage of abscission are generally smaller than persisting fruitlets, suggesting that growth arrest may precede abscission. The presence of a premature senescence phenotype in the seed coat of weakly attached fruitlets further indicates that degeneration of the seed coat may contribute to the initiation of avocado IFA (Garner and Lovatt, 2016).

The hormonal control of avocado IFA was investigated using two complementary approaches. In one study, the role of ET was examined in fruitlets on branches excised from trees when fruitlets were between 10 to 25 mm in diameter (Davenport and Manners, 1982). Under these conditions, IFA was initiated approximately three days after branch excision. Tissue degeneration within the nucellus and seed coat was observed within two days, coinciding with a marked burst in ET production primarily in the seed coat. In separate studies conducted during the summer drop period, weakly attached fruitlets, that were likely in the final stage of abscission, contained higher levels of ABA and produced more ET than persisting fruitlets (Adato and Gazit, 1977; Garner and Lovatt, 2016).

ACCEPTED MANUSCRIPT

Downloaded from https://academic.oup.com/jxb/advance-article/doi/10.1093/jxb/erag289/8709372 by Qld Dept of Employment, Economic Development & Innovation user on 19 June 2026

Despite the contribution from the above studies to avocado IFA, how fruitlets transition to abscission and whether growth arrest and seed coat senescence precede detachment and on what timescale has yet to be resolved. Further, an understanding of the early hormone signaling and developmental reprogramming that influence the fate of the seed coat to trigger abscission is lacking. To address these questions, we examined the potential role of the seed coat in avocado IFA. Specifically, we tested the hypothesis that hormone reprogramming in the seed coat initiates a senescence program of development that arrests growth and commits the fruitlet to abscission.

Materials and Methods

Plant material

Trials were conducted at well-managed orchards on three- to four-year-old 'Hass' avocado trees. The fruitlet abscission trial using digital dendrometers to evaluate whether changes in growth rate preceded abscission was performed at an orchard in the Riverland region of South Australia (-34.070312, 140.818789). The two trials used to harvest fruitlets for transcriptome and hormone analyses displayed in Fig. 1, as well as the gene-expression validation trial, were performed in south-western Western Australia (-33.63557, 115.46191). For quantifying the senescence phenotype in the seed coat, immature fruit were harvested from trees in an orchard in central Queensland (-25.05442, 152.24477).

Calculating growth rate using digital dendrometers

Digital dendrometers (Phytech, Rosh Haayin, Israel) were used to measure daily changes in the diameter of the tagged fruitlets from 73 to 129 days after full bloom (DAFB) in the Riverland orchard. At 73 DAFB, the average diameter of the tagged fruitlets was 36.5 mm. As the digital dendrometer records the diameter of a fruitlet every hour, the mean diameter of each fruitlet (mm) was calculated as the average change over 24 hrs. Growth rate (mm/day) of persisting and abscising fruitlets was calculated using the formula, growth rate = change in diameter (mm)/change in time (day). Cumulative abscission was also evaluated by scoring the percentage of fruitlets that abscised per tree over the course of the trial.

ACCEPTED MANUSCRIPT

Downloaded from https://academic.oup.com/jxb/advance-article/doi/10.1093/jxb/erag289/8709372 by Qld Dept of Employment, Economic Development & Innovation user on 19 June 2026

Experimental design for capturing normal growing and arresting fruitlets

Two trials were established at the orchard in Western Australia to identify the developmental and hormonal signaling events associated with fruitlet growth arrest.

Natural abscission trial: A total of 192 fruitlets were tagged across six trees and the diameter of each fruitlet was measured at regular time intervals using a Kincrome K11105 Digital calliper (Fig. 1A). Growth rate (mm/day) was calculated for each fruitlet over the course of the trial as described above. When the average diameter of the tagged fruitlets was 43.8 mm, six fruitlets maintaining a normal pattern of growth (NA-Normal) and six arresting fruitlets (NA-Aresting) were harvested. The mean growth rate for the sampled NA-Normal and NA-arresting were 0.49 and 0.03 mm/day, respectively. The average diameter for the NA-Normal and NA-Arresting sampled fruitlets were 42.6 and 41.6, respectively. As fruitlets were the experimental unit for our trials, each fruitlet harvested was treated as a biological replicate. After harvesting the NA-Normal and NA-Arresting fruitlets, the embryo, seed coat and pericarp tissues were separated, frozen on dry ice for RNA-sequencing and hormone quantification. Five out of six NA-Normal and NA-Arresting fruitlets were used for RNA-sequencing. For hormone quantification, all six NA-Normal and NA-Arresting fruitlets were analyzed.

Defoliation-fruitlet abscission induced trial: To capture fruitlets at an early and late stage of growth arrest, 100 fruitlets were randomly tagged across three trees, which were manually defoliated by removing the vegetative flush apical to the fruit (Fig. 1B). In parallel, 80 fruitlets were randomly tagged in three untreated-control trees. At the start of the trial, the average diameter of developing fruitlets in defoliated and untreated control trees was 36 mm. Kincrome K1105 digital callipers were used to measure the diameter of the tagged fruitlets at 0, 4, 6, and 12 days after defoliation. Growth rate (mm/day) was calculated as above. Six days after defoliation, five normal-growing fruitlets were harvested from untreated-control (UtC-Control) and defoliated trees (DEF-Early). The mean growth rates for UtC-Normal and DEF-Early fruitlets were 0.65 and 0.60 mm/day, respectively. On the same day, five arresting fruitlets (DEF-Late) with a growth rate of 0.10 mm/day were harvested. The mean diameters for UtC-Normal, DEF-Early and DEF-Late sampled fruitlets were 39.4, 38.7 and 38.3 mm, respectively. Each fruitlet was treated as a biological replicate. Embryo, seed coat and pericarp were separated and frozen on dry ice for RNA-seq. In defoliated trees, fruitlet abscission was induced between 8 and 15 days after treatment (Supplementary Fig. S1).

ACCEPTED MANUSCRIPT

Downloaded from https://academic.oup.com/jxb/advance-article/doi/10.1093/jxb/erag289/8709372 by Qld Dept of Employment, Economic Development & Innovation user on 19 June 2026

Extraction of RNA from fruit tissues

Total RNA was extracted from the seed coat, embryo, and pericarp (n = 5 for each tissue) using the Spectrum Plant Total RNA kit (Sigma-Aldrich Pty. Ltd., Sydney, NSW, Australia, #STRN250) following the manufacturer's instructions. RNA was eluted once in 50 µl of Elution Buffer, and residual DNA was removed using the TURBO DNA-free kit (ThermoFisher Scientific, Adelaide, SA, Australia, #AM1907) in a total volume of 60 µl. Library preparation and sequencing were performed by the Australian Genome Research Facility Ltd (AGRF, Melbourne, Australia) RNA sequencing service. Libraries were sequenced on an Illumina NovaSeq 6000 system (Illumina Inc, San Diego, CA, USA), generating 150 bp paired-end (PE) reads.

Transcriptomic analysis

RNA-seq libraries were prepared from seed coat, embryo, and pericarp RNA samples derived from the natural and defoliation fruit abscission trials (Fig 1A and B). Five RNA samples per tissue type were used to prepare the libraries. Across both trials, approximately ~3.15 billion PE raw reads were obtained (~ 42 million reads per library). Read quality was assessed with FastQC v0.11 (Andrews, 2010). Adapters and low-quality bases were trimmed using Trim Galore v0.6.6 (paired-end mode) (Krueger et al., 2021). Trimmed reads were aligned to the *Persea americana* cv. 'Hass' genome (Rendón-Anaya *et al.*, 2019) using STAR v2.7 (Dobin et al., 2013), and transcripts were assembled with Cufflinks v2.2.1 (Trapnell et al., 2010). Gene-level read counts were generated with HTSeq (Putri *et al.*, 2022). Transcripts were annotated by Basic Local Alignment Search Tool X (BLASTX) (Altschup *et al.*, 1990), using NCBI-blast[8] v2.10.1+ against the non-redundant protein sequence database (nr) and the Swiss-Prot protein sequence database (sp) in BLASTDB v5. Additional BLASTX runs were restricted to *Arabidopsis thaliana* (TaxID: 3702). Annotations of the 25,211 predicted genes were assigned using the top hit with E-value ≤ 1e-3, prioritizing Swiss-Prot accessions and *A. thaliana* gene descriptions where available.

Differential gene expression analysis was performed using the Bioconductor R (v. 4.0.2) package DESeq2 v.1.28.1 (Love *et al.*, 2014). Counts were normalized and differentially expressed genes (DEGs) were identified using a likelihood ratio test with adjusted $p \leq 0.05$ and $\log_2 FC \geq 1$. Variance stabilizing transformation was applied before visualisation. To identify candidate genes associated with fruitlet growth arrest, gene ontology (GO) analysis followed by Venn Diagram analysis were used to define DEGs shared between Natural Growth Arrest (NGA) and the defoliation datasets (Defoliated – Early Growth Arrest, DEGA; Defoliated – Growth Arrest, DGA) for the seed coat, pericarp and embryo (Supplementary

ACCEPTED MANUSCRIPT

Downloaded from https://academic.oup.com/jxb/advance-article/doi/10.1093/jxb/erag289/8709372 by Qld Dept of Employment, Economic Development & Innovation user on 19 June 2026

Dataset S1). Dataset S1 lists the shared DEGs related to auxin, ABA, ET, jasmonic acid (JA) homeostasis and signaling, cell cycle and cell growth, senescence and seed dormancy.

Quantitative real-time PCR

To validate the RNA-seq results, a separate trial at the Western Australia orchard was established, in which the growth rate of 73 fruitlets was evaluated across three trees using a Kincrome K11105 Digital calliper. Six persisting and six arresting fruitlets (growth rates 0.56 and 0.12 mm/d, respectively) were harvested when the cohort mean diameter was 39.5 mm (Supplementary Fig. S2). The mean diameters of the six normal-growing and six arresting fruitlets were 39.6 mm and 38.3 mm, respectively. Seed coats were isolated and pooled in pairs to generate three biological replicates per condition. Total RNA extraction followed the protocol as described above. The QuantiNova Reverse Transcription Kit (Qiagen) was used to synthesize cDNA as per manufacturer's instructions. Real-time quantitative PCR (qRT-PCR) was performed using the Rotor-Gene Q 5plex platform (Qiagen) with the QuantiNova SYBR Green PCR Master Mix (Qiagen) as per manufacturer's instructions (Qiagen: QuantiNova LNA PCR Handbook, Q-Rex Software User Manual). Two genes (*AGD12_1-like*, *ASIL2_1-like*) whose expression levels remained stable across the persisting and arresting transcriptome datasets were selected as reference genes for qRT-PCR analysis. Relative expression levels of six amplified genes were calculated using the $2^{-\Delta\Delta Ct}$ method for validation (Livak and Schmittgen, 2001), and the results were displayed in Supplementary Fig. S3. The primers used for qRT-PCR are displayed in Table S1.

Quantification of hormone metabolites

For indole-3-acetic acid (IAA) and IAA conjugated with aspartic acid (IAA-Asp) quantification, 50 mg of seed coat, pericarp and embryo samples dissected from NA-Normal and NA-Arresting fruitlets in the natural abscission trial (Fig. 1A), were ground to a fine powder in liquid nitrogen using a Cryomill (Retsch®, Haan, Germany). Six biological replicates were used for each tissue and condition, except the arresting seed coat (n=5), which was derived from five biological replicates. Hormone metabolites were extracted in 1.0 mL of ice-cold 50% (v/v) aqueous acetonitrile containing 500 pmol of deuterated IAA-d5 (Cambridge Isotope Laboratories, Andover, USA) and IAA-Asp-d5 (Böttcher et al., 2010) as previously described (Clayton-Cuch *et al.*, 2021). Briefly, after vortexing and sonicating the samples at 4^0C, the samples were centrifuged at 14,000xg and the supernatants from each sample were loaded onto a HLB-SPE cartridge (30 mg, Waters, Wexford, Ireland) pre-conditioned with methanol, nanopore water and 50% (*v/v*) acetonitrile. After collecting the flow through, the

ACCEPTED MANUSCRIPT

Downloaded from https://academic.oup.com/jxb/advance-article/doi/10.1093/jxb/erag289/8709372 by Qld Dept of Employment, Economic Development & Innovation user on 19 June 2026

cartridge was rinsed with 1.0 mL 30% (*v*/*v*) acetonitrile and the flow through and eluate were combined and dried at 50^{0}C in a vacuum concentrator (SP Genevac miVac, Ipswich, United Kingdom). Dried samples were resuspended in 50 µL of 30% (*v*/*v*) acetonitrile. IAA and IAA-Asp were analyzed by liquid chromatography coupled with tandem mass spectroscopy (LC-MS/MS) as previously described (Böttcher *et al.*, 2010; Clayton-Cuch *et al.*, 2021). Briefly, samples were analyzed on the Agilent 1260 Infinity II HPLC (Agilent, Santa Clara, CA, USA) with an Agilent 6470 Triple Quad mass spectrometer equipped with a jet stream ionization source. A Luna C18 column (75 × 4.6 mm, 5 µm; Phenomenex, Torrance, CA, USA) was used to separate metabolites after injecting 10 µL of each sample. IAA and IAA-Asp were eluted with a gradient of 0.01% formic acid in water and 0.01% formic acid in 90% (v/c) acetonitrile with a flow rate of 0.35 mL/min. Multiple reaction monitoring-mass spectrometry was used to detect IAA and IAA-Asp.

In a separate extraction, ABA, phaseic acid (PA), dihydrophaseic acid (DPA), ABA glucose ester (ABA-GE), jasmonic acid (JA) and (+)-7-iso-jasmonoyl-L-isoleucine (JA-Ile) were quantified from 50 mg of each tissue (same samples and replication as above; Fig. 1A). The extraction followed the protocol described above with internal standards added during extractions for quantifications: 5 ng of d6-ABA, d3-PA, d3-DPA and d5-ABA-GE (National Research Council Canada, Saskatchewan, Canada) plus 250 pmol of d5-JA and 25 pmol of d2-JA-Ile (OlChemIm Ltd., Olomouc, Czech Republic).

For ACC quantification, a third extraction (50 mg tissue, same samples and replication as above) was performed as described above with ACC-d4 added as internal standard. Using the same LC-MS/MS system as described above, ACC was quantified by injecting 2 µL of the same extract onto a HILIC-Z column (Poroshell 120 HILIC-Z 2.1 x 100mm 2.7 µm, Agilent, USA) heated to 30^{0}C. At 7.4 min with a flow rate of 0.2 mL/min, ACC and its internal standard ACC-d4 (OlChemIm Ltd., Olomouc, Czech Republic) were eluted with 20 mM ammonium formate in water (eluent A) and a gradient of 20 mM ammonium formate in 90% (v/c) acetonitrile (eluent B): 100-30% B (0-10 min), 30% B (10-15 min), and 100% B (15-20 min).

Quantification of the senescence phenotype in the seed coat during growth arrest

A population of fruitlets (*n*=127) was tagged with digital dendrometers (Phytech, Rosh Haayin, Israel) across 14 trees at the Queensland orchard to monitor fruitlet growth. To characterize the timing of seed coat senescence, fruitlets with growth rates ranging from -1.15 to 0.74 mm/day were sampled. The sampled fruitlets were further categorized based on

ACCEPTED MANUSCRIPT

Downloaded from https://academic.oup.com/jxb/advance-article/doi/10.1093/jxb/erag289/8709372 by Qld Dept of Employment, Economic Development & Innovation user on 19 June 2026

their pattern of growth (mm/day) during the 10 days prior to harvest. After sampling, each fruitlet was cut in half, the embryo removed, and both seed-coat halves were imaged side by side at a fixed distance. The senescence phenotype was quantified via image analysis using the FIJI image processing package (version 1.53c; Schindelin *et al.,* 2012). Briefly, the polygon tool was used to accurately outline and select each seed coat half before a consistent colour threshold was applied, with minimum and maximum values for Hue (5 to 101), Saturation (101-255) and Brightness (150-255), to isolate the area of senescence. Threshold area plus total seed coat half area was quantified and percent area in pixels was calculated for each seed coat half to derive the percent senescence phenotype for the seed coat from each fruitlet.

Statistical analysis

Differentially expressed genes with significant changes in transcript levels between normal growing and arresting fruitlets were identified in in seed-coat, pericarp and/or embryo using a likelihood ratio test in DESeq2, with adjusted $p \leq 0.05$ and $\log_2 FC \geq 1$. For physiological and image-analysis data, Student's t-tests and one-way ANOVA with Tukey's honestly significant difference (HSD) were performed in GraphPad Prism v10.4.1. Unless otherwise stated, tests were two-tailed and significance thresholds were set at $p \leq 0.05$.

Results

Fruitlets undergo growth arrest prior to abscission

To better understand how immature fruit transition from a phase of growth to abscission, we investigated whether a change in the rate of growth preceded abscission. Digital dendrometers were utilized to characterize the daily growth patterns of developing fruitlets starting from 73 days after full bloom (DAFB) when the average fruitlet diameter was 36.5 mm (Fig. 2A). Over the course of the trial, the average diameter of developing fruitlets increased at a steady rate. At the beginning of the trial, the mean growth rate of persisting fruitlets from 73 to 79 DAFB was 0.57 mm/d (Fig. 2B). At the end of the trial, the mean growth rate from 123 to 129 DAFB declined to 0.32 mm/d, when the average diameter of the fruitlet was 62.3 mm. Fruitlet abscission occurred continuously, with trees dropping an average of 47.4% of fruitlets by the end of the trial (Fig. 2C). The peak of fruitlet abscission coincided with an average fruitlet diameter of 46.6 mm (Fig. 2D). The growth rate of fruitlets that abscised over the course of this trial was collated and plotted against days to fruit drop (Fig. 2E). Results showed that fruitlets fated to abscise underwent growth arrest before they shrunk and abscised from the tree (note: detachment occurred on day zero). The slowing

ACCEPTED MANUSCRIPT

Downloaded from https://academic.oup.com/jxb/advance-article/doi/10.1093/jxb/erag289/8709372 by Qld Dept of Employment, Economic Development & Innovation user on 19 June 2026

and eventual cessation of fruitlet growth took approximately 6-days plus another four- to six-days for the shrinking fruitlet to abscise.

The transcriptome of maternal organs is highly responsive to fruitlet growth arrest

To gain insight into the developmental basis of fruitlet growth arrest under natural conditions, transcriptomes were generated for the seed coat, pericarp and embryo samples derived from five actively growing (NA-Normal) fruitlets and five immature fruit sampled at a late stage of growth arrest (NA-Arresting) (Fig. 1A). In an independent trial, defoliation was used to induce IFA, which caused an average 97% of the fruitlets to abscise (Supplementary Fig. S1). As fruitlets underwent growth arrest prior to abscission after defoliation (Supplementary Fig. S1), we used this inducible system to capture fruitlets at an early and late stage of growth arrest (Fig. 1B). Specifically, five immature fruitlets that maintained a normal growth rate, but expected to undergo growth arrest, were sampled six-days after defoliation to identify transcriptomes associated with early growth arrest (DEF-Early; Fig. 1B). At this time point, five fruitlets whose growth rate switched from a normal to a low growth rate were also collected to identify transcriptomes associated with late growth arrest (DEF-Late; Fig. 1B). In parallel, five normal growing fruitlets were sampled from untreated control trees (UtC-Normal) at the same time when DEF-Early and DEF-Late fruits were collected. Subsequently, transcriptomes for the seed coat, pericarp and embryo were generated from the five DEF-Early, DEF-Late and UtC-Normal fruitlets (Fig. 1B).

Principal component analysis (PCA) for the seed coat, pericarp and embryo transcriptomes derived from the natural (NA-Normal and NA-Arresting) and defoliation-induced (DEF-Early, DEF-Late and UtC-Normal) abscission trials showed that normal growing (NA-Normal and UtC-Normal) and arresting (NA-Arresting, DEF-Early and DEF-Late) tissue samples were primarily separated by the first two principal components, which explained 52% and 23% of the variance in the dataset (Fig. 3A). The variance between the normal growing and arresting seed coat and pericarp transcriptomes under natural conditions and in response to defoliation was substantially higher compared to the variance within the embryo transcriptomes. Notably, transcriptomes for NA-Arresting and DEF-Late samples, which captured fruitlets at a late stage of growth arrest, clustered together (Fig. 3A). PCA also showed that the maternal transcriptomes of DEF-Early clustered along an axis that was more closely positioned to the UtC-Normal than the DEF-Late transcriptomes for the seed coat and pericarp. Further, the DEF-Early seed coat transcriptome displayed a greater degree of variance compared to the DEF-Early pericarp transcriptome (Fig. 3A). The clustering of the

ACCEPTED MANUSCRIPT

Downloaded from https://academic.oup.com/jxb/advance-article/doi/10.1093/jxb/erag289/8709372 by Qld Dept of Employment, Economic Development & Innovation user on 19 June 2026

NA-Normal and UtC-Normal seed coat, pericarp and embryo transcriptomes was expected, as these two sets of fruitlets were harvested 14-days apart from each other (Fig. 3A).

To better understand the transcriptional dynamics associated with a fruit growth cessation, differentially expressed genes (DEGs) associated with a late stage of natural growth arrest (NGA) were identified by comparing the transcriptome of NA-Normal with NA-Arresting for the seed coat, pericarp and embryo (Fig. 3B). The temporal changes in gene expression profiles were identified by comparing the seed coat, pericarp and embryo transcriptomes derived from UtC-Normal with DEF-Early and DEF-Late. By comparing UtC-Normal with DEF-Early transcriptomes, DEGs associated with early growth arrest in response to defoliation were identified (Defoliation Early Growth Arrest, DEGA; Fig. 3C). Likewise, comparing UtC-Normal with DEF-Late transcriptomes was used to identify DEGs associated with a late stage of growth arrest in response to defoliation (Defoliation Growth Arrest, DGA; Fig. 3D).

Venn diagram analysis was used to identify core sets of DEG implicated in fruitlet growth arrest (Fig. 3E-G). From this analysis, we identified 2303, 1059 and 711 DEGs in the seed coat, pericarp and embryo, respectively, that were shared between NGA, DGA and DEGA (Fig. 3E-G). DEGs shared between DEGA and NGA were used to identify a core set of genes implicated in early growth arrest. Here, 2556, 1147 and 789 DEGs implicated in early growth arrest were detected in the seed coat, pericarp and embryo, respectively. The total number of shared DEGs between NGA and DGA, which represent a core set of genes implicated in a late growth arrest, were 7897, 6158 and 2451 for the seed coat, pericarp and embryo, respectively (Fig. 3E-G). As hormones play a critical role in regulating fruit growth and development (Kumar *et al.*, 2014; Fenn and Giovannoni, 2021), as well as senescence (Pautot *et al.*, 2025), DEGs implicated in auxin, ABA, ET and JA homeostasis and signaling were identified in the core sets of DEGs implicated in early and late stages of growth arrest in seed coat, pericarp and embryo.

A reduction in auxin activity is associated with fruitlet growth arrest

As indole-3-acetic acid (IAA) is the major form of auxin that regulates fruit development (Kumar *et al.*, 2014; Fenn and Giovannoni, 2021), we investigated whether growth arrest was associated with changes in the expression of genes that regulate IAA homeostasis in the seed coat, pericarp and embryo. IAA production is controlled in part by a two-step pathway, in which tryptophan is converted to indole-3-pyruvic acid (IPA) via TRYPTOPHAN

ACCEPTED MANUSCRIPT

Downloaded from https://academic.oup.com/jxb/advance-article/doi/10.1093/jxb/erag289/8709372 by Qld Dept of Employment, Economic Development & Innovation user on 19 June 2026

AMINOTRANSFERASE OF ARABIDOPSIS (TAA) and TAA-RELATED (TAR; Fig. 4A) (Mashiguchi *et al.*, 2011; Won *et al.*, 2011). In the second step of this pathway, the rate limiting YUCCA (YUC) flavin monooxygenase-like enzymes catalyse the conversion of IPA to IAA. In addition to IAA biosynthesis, free IAA is also controlled in part by GRETCHEN HAGEN 3 (GH3) acyl acid amido synthetases, which conjugate IAA with aspartic acid (Asp), as well as other amino acids, to store, transport or inactivate this hormone (Fig. 4A) (Staswick *et al.*, 2005).

To investigate a potential role for auxin in fruitlet growth arrest, Gene Ontology (GO) analysis was used to identify *TAA/TAR-like*, *YUC-like* and *GH3-like* genes whose expression changed in response to growth arrest. Results showed that *YUC4-like* and *YUC6-like* genes were downregulated at late stages of growth arrest in the seed coat and pericarp (Fig. 4B; Supplementary Fig S4). Moreover, the levels of *YUC4-like* and *YUC6-like* were repressed early in the growth arrest process in the seed coat compared to the pericarp (Fig. 4B; Supplementary Fig. S4). In contrast to *YUC4-like* and *YUC6-like*, no *TAA*/*TAR*-like genes were identified as a DEG during growth arrest in the seed coat and pericarp (Supplementary Dataset S1). In response to growth arrest, *GH3.1-like* genes were differentially expressed in the maternal organs (Fig. 4C; Supplementary. Fig S4). *GH3.1-like_1/3* were upregulated in the seed coat at early and late stages of growth arrest; whereas, only *GH3.1-like_1* increased in the pericarp at late growth cessation. In addition, *GH3.1-like_2* and *DFL2-like* were down-regulated in the maternal organs during growth arrest (Fig. 4C; Supplementary. Fig S4). In the embryo, none of the TAA/*TAR-like* and *YUC-like* genes were identified as DEGs (Supplementary Dataset S1), while *GH3.1-like1/3* were upregulated during late growth arrest (Fig. 4C; Supplementary Fig. S4). Genes that encode auxin transporters and response transcription factors were also differentially expressed, predominantly in maternal tissues and to a lesser extent in the embryo (Supplementary Fig. S5 and S6).

To further address a potential role for auxin in IFA, the levels of IAA and IAA-Asp were quantified in the seed coat, pericarp and embryo of NA-Normal and NA-Arresting fruitlets. Results showed that in NA-Normal fruitlets, IAA was 11.4- and 10.2-fold higher in the seed coat than in the pericarp and embryo, respectively (Fig. 4D). At a late stage of growth arrest, IAA levels were significantly reduced in the seed coat (p=0.006) and pericarp (p=0.004) of NA-Arresting compared to NA-Normal fruitlets (Fig. 4D). To determine if auxin conjugation was associated with a decrease in free IAA levels at a late stage of growth arrest, the levels of IAA-Asp were quantified in the seed coat and pericarp, and embryo in NA-Normal and NA-Arresting fruitlets (Fig. 4E). Results showed that level of IAA-Asp increased 7.3-fold in the seed coat of NA-Arresting (p=0.006) compared to NA-Normal fruitlets. While the average

ACCEPTED MANUSCRIPT

Downloaded from https://academic.oup.com/jxb/advance-article/doi/10.1093/jxb/erag289/8709372 by Qld Dept of Employment, Economic Development & Innovation user on 19 June 2026

level of IAA-Asp increased in the pericarp in NA-Arresting compared to NA-Normal fruitlets, this trend was not statistically significant (p=0.13). In the embryo, there were no differences in the levels of IAA and IAA-Asp between NA-Normal and NA-Arresting fruitlets (Fig. 4D and E).

Accumulation of ABA in the maternal organs is associated with fruitlet growth cessation

As ABA is implicated in avocado IFA (Adato and Gazit, 1977; Garner and Lovatt, 2016), we investigated whether an increase in ABA activity in the seed coat, pericarp and/or embryo was associated with growth arrest. ABA is synthesized from the C_{40}-carotenoid precursors, 9-*cis*-neoxanthin and 9-*cis*-violaxantin, in a three-step process mediated by 9-*cis*-expoxycarotenoid dioxygenase (NCED), a short-chain alcohol dehydrogenase (ABA2) and abscisic acid aldehyde oxidase (AAO3; Fig. 5A) (Chen et al., 2020).

To investigate a potential role for ABA in growth arrest, GO analysis was used to identify DEGs involved in ABA biosynthesis and catabolism. In the seed coat, the expression of *NCED9/3-like* and *AAO3-like* genes increased during early and late stages of growth arrest (Fig. 5B; Supplementary Fig. S7). In addition, *AAO3-like_1/2* increased at late growth arrest in the seed coat. In the pericarp, ABA biosynthesis genes were differentially expressed with *NCED9/3-like*, *ABA2-like* and *AAO3-like* genes upregulated and/or downregulated during growth arrest (Fig. 5B; Supplementary Fig. S7). In the pericarp, *AAO3-like_1/2* were upregulated during early and late stages of growth arrest. In contrast to the maternal organs, the only ABA biosynthesis gene that was differentially expressed in the embryo during growth cessation was *NCED3-like_2*, which was upregulated (Fig. 5B; Supplementary Fig. S7).

In *Arabidopsis* and maize, experimental studies indicate that the HOMEOBOX PROTEIN 40 (HB40)/GRASSY TILLERS1 (GT1) transcription factor inhibits bud outgrowth in part by inducing *NCED* gene expression (Fig. 5A) (Gonzalez-Grandio *et al.*, 2017; Dong *et al.*, 2019). Consistent with this regulatory role, *HB40-like(s)* genes were upregulated in the seed coat and pericarp at early and late stages of growth arrest (Fig. 5B; Supplementary Fig. S7). In contrast, no *HB40-like* was identified as DEG in the embryo (Supplementary Dataset S1).

ABA catabolism is a two-step process in which ABA is first converted to phaseic acid (PA) by CYP707A cytochrome P450 monooxygenases (Fig. 5C) (Kushiro *et al.*, 2004; Saito *et al.*, 2004). Subsequently, PHASEIC ACID REDUCTASE (PAR) catalyses PA to dihydrophaseic acid

ACCEPTED MANUSCRIPT

Downloaded from https://academic.oup.com/jxb/advance-article/doi/10.1093/jxb/erag289/8709372 by Qld Dept of Employment, Economic Development & Innovation user on 19 June 2026

(DPA) (Weng *et al.*, 2016). In the seed coat, *CYP707A1/2-like* were upregulated during early and late stages of growth arrest (Fig. 5D; Supplementary Fig. S8). In contrast, the increased expression of *CYP707A1/2-like* in the pericarp occurred only during a late stage of growth arrest. In the embryo, *CYP707A2-like* was induced at early and later stages of growth arrest, while *CYP707A1-like* increased at a late stage of growth cessation (Fig. 5D; Supplementary Fig. S8). In the GO analysis, a gene(s) encoding a PAR-like enzyme was no identified in the DEGs associated with ABA biosynthesis and catabolism (Supplementary Dataset S1).

To further examine the association of ABA with fruit growth arrest, the levels of this hormone, as well as PA and DPA, were quantified in the seed coat, pericarp and embryo isolated from NA-Normal and NA-Arresting fruitlets. In NA-Normal fruitlets, ABA was relatively low in the seed coat compared to the pericarp and embryo (Fig. 5E). At a late stage of growth arrest, ABA increased significantly in the seed coat (p=0.009) and pericarp (p=0.008) but not in the embryo of NA-Arresting compared to NA-Normal fruitlets (Fig. 5E). In the maternal organs derived from NA-Normal fruitlets, the levels of PA were low compared to the embryo (Fig. 5F). In NA-Arresting fruitlets, a significant increase in PA occurred in the seed coat (p=0.011) and pericarp (p=0.011) compared to NA-Normal fruitlets (Fig. 5F). DPA levels were highest in the pericarp of NA-Normal fruitlets (Fig. 5G) and increased significantly in pericarp (p=0.035) and embryo (p=0.031) in NA-Arresting fruitlets (Fig. 5G). While conjugation of ABA with glucose to form the ABA-glucose ester (ABA-GE) regulates the activity and localization of this hormone (Chen et al., 2020), results showed that there was no significant change in the levels of ABA-GE in the seed coat, pericarp and embryo in NA-Arresting compared to NA-Normal (Supplementary Fig. S9).

ACC increased in the seed coat during growth arrest

As ET is implicated in avocado IFA (Adato and Gazit, 1977; Davenport and Manners, 1982), we investigated whether the precursor, ACC, used as a proxy for ET, accumulated in the seed coat, pericarp and/or embryo during growth arrest. ET is produced by a two-step biosynthetic process starting with S-adenosyl-L-methionine (SAM), which is converted to 1-aminocyclopropane-1-carboxylic acid (ACC) via ACC synthase (ACS; Fig. 6A) (Pattyn et al., 2021). In the second step, conversion of ACC to ET is mediated by ACC oxidase (ACO). GO analysis was used to identify DEGs involved in ET biosynthesis during growth arrest (Fig. 6B; Supplementary Fig. S10). Results showed that *ACS1-like_1* and *ACS1-like_7* were upregulated during early and late stages of growth arrest in the seed coat (Fig. 6B; Supplementary Fig. S11). In addition, the expression of *ACS1-like_2* increased at late growth arrest in the seed coat. In the pericarp and embryo, transcript abundance for *ACS1-like_1*

ACCEPTED MANUSCRIPT

Downloaded from https://academic.oup.com/jxb/advance-article/doi/10.1093/jxb/erag289/8709372 by Qld Dept of Employment, Economic Development & Innovation user on 19 June 2026

increased during early and late stage of growth arrest. The expression of *ACS7-like* increased during late growth arrest in the pericarp. In contrast to the seed coat and embryo, only the pericarp displayed an upregulation of an *ACO* gene, *ACO4-like*, during growth arrest (Fig. 6B; Supplementary Fig. S10).

A role for ACC in IFA was evaluated by quantifying the levels of this metabolite in the seed coat, pericarp and embryo in NA-Normal and NA-Arresting fruitlets. Results showed that ACC accumulated in the seed coat, pericarp and embryo in NA-Normal fruitlets (Fig. 6C). In NA-Arresting fruitlets, a significant increase in ACC levels only occurred in the seed coat (Fig. 6C, $p<0.001$) compared to NA-Normal fruitlets. In the embryo, despite the upregulation of *ACS1-like_1* (Fig. 6B), the levels of ACC were significantly lower in NA-Arresting fruitlets compared to NA-Normal fruitlets ($p=0.006$; Fig. 6C).

An increase in jasmonate levels in the seed coat during fruit growth arrest

Since JA negatively regulates growth and promotes senescence (Huang *et al.*, 2017; Guo *et al.*, 2018), we examined whether this hormone was associated with avocado fruitlet growth arrest. The production of JA from alpha-linolenic acid is a multistep process mediated by 13-lipoxygenase (LOX), allene oxide synthase (AOS), allene oxide cyclase (AOC), and 12-oxophytodienoic acid reductase (OPR; Fig. 7A) (Huang *et al.*, 2017). In the final step, JASMONATE RESISTANT 1 (JAR1) conjugates JA with isoleucine (Ile) to produce the bioactive jasmonate, jasmonoyl-isoleucine (JA-Ile) (Staswick and Tiryaki, 2004). To investigate a possible role for JA in fruitlet growth arrest, GO analysis was used to identify DEGs involved in JA biosynthesis (Fig. 7B; Supplementary Fig. S11). Results showed that *LOX4-like*, *LOX5-like_1* and *AOS-like_2/3/4* were upregulated in the seed coat during early and late stages of growth arrest (Fig. 7B; Supplementary Fig. S11). In addition, transcript levels for *LOX2-like_2* and *LOX5-like_2/3* also increased during late growth arrest in the seed coat. In contrast, during late growth arrest, *AOC3-like* and *AOC4-like* were downregulated (Fig. 7B; Supplementary Fig. S11). JA biosynthesis genes were also differentially expressed in the pericarp and embryo but to a lesser extent than the seed coat during growth cessation (Fig. 7B; Supplementary Fig. S11). Despite the overall up-regulation of *LOX-like*, *AOS-like* and *AOC-like* in the seed coat, as well as the pericarp and embryo, no *JAR1-like* genes were identified as a DEG by GO analysis in these fruit tissues during growth arrest (Supplemental Dataset 1).

ACCEPTED MANUSCRIPT

Downloaded from https://academic.oup.com/jxb/advance-article/doi/10.1093/jxb/erag289/8709372 by Qld Dept of Employment, Economic Development & Innovation user on 19 June 2026

To determine if an increase in JA is associated with fruitlet growth cessation, the levels of JA and the bioactive form of this hormone, (+)-7-iso-jasmonoyl-L-isoleucine (JA-Ile) (Fonseca et al., 2009), were quantified in the seed coat, pericarp and embryo of NA-Normal and NA-Arresting fruitlets. Results showed JA was detected in the seed coat, pericarp and embryo in NA-Normal fruitlets (Fig. 7C). At a late stage of growth arrest, JA significantly increased in the seed coat of NA-Arresting compared to NA-Normal fruitlets (p = 0.002). A modest but significant increase in JA also occurred in the pericarp (p = 0.014); whereas, the level of this hormone in the embryo remained unchanged in NA-Arresting compared to NA-Normal fruitlets (Fig. 7C). JA-Ile was extremely low in all tissues of NA-Normal fruitlets (Fig. 7D), but increased significantly in the seed coat of NA-Arresting fruitlets (p = 0.001), with no significant changes in pericarp (p = 0.55) or embryo (p = 0.14; Fig. 7D).

Seed coat senescence is initiated at a late growth arrest

In fruitlets with a mean growth rate > 0.40 mm/day, the seed coat was yellowish in appearance with punctate browning restricted to the vascular connections at the base of this maternal organ (Fig. 8A, red arrowhead). In contrast, abscised fruitlets displayed a senescence phenotype in seed coat (Fig. 8B). To determine the timing of seed coat senescence in the IFA pathway, image analysis was used to quantify the senescence phenotype in the seed coat of actively growing, arresting and shrinking fruitlets when the average diameter of the fruitlets was approximately 51 mm in diameter. Here, fruitlets were grouped together based on their growth rate at the time of sampling, as well as their overall pattern of growth ten days before harvest (Supplementary Fig. S12). Results showed the mean senescence phenotype in the seed coat of fruitlets that maintained a relatively consistent pattern of growth and a growth rate ≥ 0.3 mm/day was < 0.7% (Fig. 8C; Supplementary Fig. S12). Fruitlets sampled with a growth rate between 0.2 to 0.29 mm/day, which displayed a similar pattern of growth as fruitlets harvested with a growth rate ≥ 0.3 mm/day, also showed a mean senescence phenotype in the seed coat < 0.7% (Fig. 8C; Supplementary Fig. S12). To identify fruitlets that appeared to be committed to abscission, immature fruit with growth rates ≤ 0.2 mm/day, which displayed a decline in growth for three days, were harvested and the senescence phenotype of the seed coat was evaluated (Supplementary Fig. S12). Results showed that fruitlets with growth rate between 0.1 to 0.19 mm/day displayed a minimal mean senescence phenotype less than < 1.0% (Fig. 8C). Although fruitlets with growth rates of 0.00 to 0.09 mm/day displayed a mean senescence value of 4.9%, this was not statistically different with fruitlets that had a growth rate > 0.1 mm/day (Fig. 8C). In contrast, fruitlets exhibiting negative growth rates showed a significant increase in the seed coat senescence phenotype (Fig. 8C).

ACCEPTED MANUSCRIPT

Downloaded from https://academic.oup.com/jxb/advance-article/doi/10.1093/jxb/erag289/8709372 by Qld Dept of Employment, Economic Development & Innovation user on 19 June 2026

To further characterize the timing of seed coat senescence phenotype at the molecular level, GO analysis was used to identify DEGs that encode positive and negative regulators of senescence (Fig. 8D). For example, senescence-associated genes such as *AUXIN RESPONSE FACTOR1* (*ARF1-like*), *PHYTOALEXIN DEFICIENT4-like* (*PAD4*-like), *BIFUNCTIONAL NUCLEASE1* (*BFN1*), *SENESCENCE ASSOCIATED GENE 12* (*SAG12*), *ARABIDOPSIS A-FIFTEEN* (*AAF*) and *SMALL AUXIN UP RNA 36* (*SAUR36*), are often used as markers to evaluate the onset and progression of senescence (Noh and Amasino, 1999; Morris *et al.*, 2000; Pérez-Amador *et al.*, 2000; Ellis *et al.*, 2005; Chen *et al.*, 2012; Hou *et al.*, 2013). Results showed that *PAD4*-like and *ARF1-like* were upregulated during early and late stages of growth arrest in the seed coat (Fig. 8D; Supplementary Fig. S13). However, most senescence-associated genes that positively regulate tissue degeneration, including *BFN1-like*, *SAG12*-like, *AAF-like* and *SAUR36-like*, were upregulated during late growth arrest. In addition, transcript abundance for genes homologous to *JUNGBRUNNEN1* (*JUB1*) and WRKY70, which are induced during senescence but negatively regulate this process (Besseau *et al.*, 2012; Wu *et al.*, 2012), increased during growth arrest (Fig. 8D; Supplementary Fig. S13). A subset of senescence-associated genes were also upregulated in the pericarp and embryo during late growth arrest (Supplemental Dataset S1). However, in contrast to the seed coat, the pericarp and embryo displayed little or no visible signs of senescence (Fig. 8B and 9B). In addition to senescence associated genes, ET- and JA-signaling genes implicated in senescence were differentially expressed during fruitlet growth arrest (Supplementary Fig. S14 and S15).

Late growth arrest is associated with transcriptional changes implicated in seed dormancy

In persisting and recently abscised avocado fruitlets, the embryo displayed no visible signs of tissue degeneration (Fig. 9A and B). Whereas, the seed coat of abscised fruitlet displayed visible signs of senescence (Fig. 9B, red arrowhead). With the apparent absence of tissue degeneration in the embryo, we speculated that the seed may have undergone a dormancy-like program of development during growth arrest. As seed dormancy is positively regulated in part by ABA signaling derived from maternal organs and zygotic tissues (Iwasaki et al., 2022 Chen et al., 2020), GO analysis was used to identify DEGs involved in ABA and dormancy-associated signaling pathways. In the seed coat, pericarp and embryo, at least one gene encoding an ABA receptor, termed PYRABACTIN RESISTANCE (PYR)/PYR-LIKE (PYL), was induced in response to growth cessation (Fig. 9D; Supplementary Fig. S16). For example, *PYL9-like_2, PYL8-like* and *PYL4-like_1* were upregulated during early and late

ACCEPTED MANUSCRIPT

Downloaded from https://academic.oup.com/jxb/advance-article/doi/10.1093/jxb/erag289/8709372 by Qld Dept of Employment, Economic Development & Innovation user on 19 June 2026

stages of growth arrest in the seed coat. In the embryo, only *PYL4-like_1* was also upregulated during early and late stages of growth arrest. During growth cessation, the expression of at least one gene that encoded a SUCROSE NONFERMENTING-1-RELATED KINASE 2.6 (SnRK2.6), which positively regulates ABA signaling (Chen et al., 2020), increased in the seed coat, pericarp and embryo (Fig. 9D; Supplementary Fig. S16). For example, in the seed coat and embryo, *SnRK2.6-like_5* was upregulated during late growth arrest. In addition, transcript levels for *SnRK2.6-like_2* increased during early and late stages of growth arrest, while *SnRK2.6-like_6* was only upregulated at late growth arrest in the seed coat (Fig. 9D; Supplementary Fig. S16). In the maternal organs, growth arrest was also associated with the upregulation of *ABA INSENSITIVE 1-like_1* (*ABI1-like_1*) and *ABA-RESPONSIVE ELEMENT BINDING FACTOR2-like* (*ABF2-like*) (Fig. 9D; Supplementary Fig. S16). In contrast to *ABI-like_1*, *ABI3-like* was downregulated in the pericarp during growth arrest (Fig. 9D; Supplementary Fig. S16). In the embryo, no *ABI-like* or *ABF2-like* genes were identified as a DEG by GO analysis during growth arrest (Supplemental Dataset 1).

In addition to ABA signaling, the dormancy potential of a seed is also influenced by FLOWERING LOCUS T (FT) in the seed coat, which acts to delay seed dormancy (Fig. 9C) (Chen *et al.*, 2014). In contrast to FT, MOTHER OF FT AND TFL1 (MFT) acts in the embryo to promote dormancy in part by modulating ABA signaling (Fig. 9C) (Xi *et al.*, 2010; Nakamura *et al.*, 2011; Footitt *et al.*, 2017). Results from our study showed that the expression of *FT-like_1/2* were downregulated during growth arrest in the seed coat and pericarp (Fig. 9E; Supplementary Fig. S17). In these maternal organs, *MFT-like_2* was also suppressed during growth arrest (Fig. 9F; Supplementary Fig. S17). However, *MFT-like_3* was upregulated at late growth arrest in the seed coat. In contrast to the seed coat and pericarp, *MFT-like_1/2* were upregulated in the embryo during late growth arrest (Fig. 9E; Supplementary Fig. S17).

Discussion

Origin of the IFA signal

The seed coat plays a critical role in regulating seed and fruit development (Radchuk and Borisjuk, 2014; Figueiredo and Köhler, 2018; Robert, 2019). For example, experimental studies indicate that signals derived from the seed coat regulate embryo patterning, seed maturation and dormancy (Radchuk and Borisjuk, 2014; Robert *et al.*, 2018; Iwasaki *et al.*, 2022). Based on the senescence phenotype displayed in the seed coat, we hypothesized that this maternal organ plays a critical role in avocado IFA. Consistent with this hypothesis, transcriptome reprogramming induced during avocado fruitlet growth arrest was

ACCEPTED MANUSCRIPT

Downloaded from https://academic.oup.com/jxb/advance-article/doi/10.1093/jxb/erag289/8709372 by Qld Dept of Employment, Economic Development & Innovation user on 19 June 2026

substantially greater in the seed coat and pericarp compared to the embryo. Further, during early growth arrest, the seed coat exhibited a greater number of DEGs than the pericarp and embryo. Together, these results indicate that the seed coat is the maternal organ that perceives and transmits the IFA signal(s) to the pericarp and embryo to coordinate developmental programs required for abscission. It is highly conceivable that this IFA signaling event(s) transmitted from the seed coat to induce growth arrest is mediated in part by a signal(s) that mediates the transition from growth to senescence, as well as the activation of a dormancy-like pathway in the seed.

If the seed coat is the site where IFA signaling is initiated, what is the nature of this signal(s)? Experimental studies indicate that auxin increases in the seed coat upon fertilization, where it regulates embryo and seed development (Robert *et al.*, 2018; Robert, 2019). As seed derived auxin is thought to regulate fruit development (Robert, 2019; Fenn and Giovannoni, 2021), the movement of auxin from the seed coat to the pericarp may also act to coordinate growth of the fruit tissues. Further, a reduction of auxin activity is key for organs to acquire the competence to undergo senescence and abscission (McAtee *et al.*, 2013; Mueller-Roeber and Balazadeh, 2014; Patharkar and Walker, 2019; Fenn and Giovannoni, 2021). Results from our study indicate that the seed coat is the primary site of IAA production in developing avocado fruitlets during summer IFA event. This is supported by data showing that IAA is 10- to 11-fold higher in the seed coat than in the pericarp and embryo, respectively. Further, at a late stage of fruitlet growth arrest, free IAA levels were significantly reduced in the seed coat. In addition, the seed coat exhibited changes in auxin biosynthesis (*YUC4/6-like*) and IAA-conjugation (*GH3.1-like_1*) genes earlier in the growth arrest process than the pericarp. Lastly, the decrease in free IAA in the seed coat during growth arrest may ultimately reduce the export and polar transport of auxin through the pedicel to allow ET to promote cell separation and detachment. Together, we hypothesize that the reduction in seed coat auxin levels is the primary signaling event that is transmitted to the pericarp and embryo to induce growth cessation and commit the arrested fruitlet to abscission.

Growth arrest is an initial step in the avocado fruitlet abscission pathway

Studies in avocado and apple indicate that a slowing of fruitlet growth precedes abscission (Ward and Marini, 1999; Greene *et al.*, 2013; Garner and Lovatt, 2016). Under natural conditions and in response to defoliation, our results showed that fruitlets fated to abscise undergo growth arrest before shrinking and detaching from the tree. The manifestation of the growth arrest phenotype early in the avocado IFA pathway, is further supported by the fact that a substantial number of genes that regulate growth were differentially expressed in the

ACCEPTED MANUSCRIPT

Downloaded from https://academic.oup.com/jxb/advance-article/doi/10.1093/jxb/erag289/8709372 by Qld Dept of Employment, Economic Development & Innovation user on 19 June 2026

seed coat, pericarp and embryo (Supplementary Dataset S1), including the overall downregulation of genes that regulate cell cycle progression (Supplementary Fig. S18). Therefore, we hypothesize that the proposed feedback interactions between expanding shoots and developing fruitlets (Sawicki *et al.*, 2015), as well as among immature fruit (Sadka *et al.*, 2023), that mediate IFA act to inhibit growth before fruitlets detach from the tree.

As auxin plays a fundamental role in mediating cell division and expansion during the growth phase of fruit development (Kumar *et al.*, 2014; Fenn and Giovannoni, 2021), our results suggest that reduced auxin activity in the seed coat and pericarp plays a key role in fruitlet growth arrest. In the seed coat and pericarp, this change in auxin activity was also accompanied with an increase in ABA, in which the latter hormone can function as an inhibitor of growth (Chen *et al.*, 2020). Indeed, the seed coat and pericarp of arresting fruitlets exhibited an overall upregulation of ABA biosynthesis genes during growth arrest. Although ABA did not increase in the embryo during growth arrest, upregulation of *NCED-like_2* together with elevated levels of DPA suggests that ABA may be produced but rapidly degraded. The significant increase in PA and/or DPA in the maternal organs suggests that ABA was tightly regulated during growth arrest. It is likely that ABA catabolism was mediated in part by the upregulation of *CYP707A1-like* and *CYP707A2-like* at early and/or late stages of growth arrest. These results are consistent with previously published studies showing that weakly attached avocado fruitlets in the final stage of abscission displayed elevated levels of ABA in the pericarp (Adato and Gazit, 1977; Garner and Lovatt, 2016). Further, application of ABA to immature avocado fruit suppressed growth (Moore-Gordon *et al.*, 1998). Taken together, we speculate that an increase in ABA in the maternal organs in response to reduced auxin activity functions to suppress growth. Given that ET and JA signaling can also suppress growth (Dubois *et al.*, 2018; Guo *et al.*, 2018), the increase of ACC and JA/JA-Ile together with ABA may collectively function to inhibit fruitlet growth when auxin activity is reduced in the seed coat and pericarp.

A potential role of seed coat senescence in avocado fruitlet abscission

Seed coat senescence is a prominent phenotype displayed in abscised avocado fruitlets (Salazar-Garcia *et al.*, 2013) (Fig 8). To evaluate whether seed coat senescence is activated upstream of fruitlet detachment, we investigated the timing of this degenerative process during fruitlet growth arrest. Our results indicate that seed coat senescence is induced at a late stage of growth arrest and becomes visibly apparent when fruitlets shrink just prior to abscission. This is supported by the fact that molecular markers of senescence, such as *SAUR36-like_2*, *SAG12-like*, *BFN1-like* and *AAF-like*, are induced at a late stage of growth

ACCEPTED MANUSCRIPT

Downloaded from https://academic.oup.com/jxb/advance-article/doi/10.1093/jxb/erag289/8709372 by Qld Dept of Employment, Economic Development & Innovation user on 19 June 2026

arrest before visible signs of senescence. The overall upregulation of genes encoding positive and negative regulators of senescence at late growth arrest further indicates that this degenerative process is highly regulated. As senescence typically precedes abscission (Patharkar and Walker, 2019; Pautot *et al.*, 2025), our results suggest that seed coat senescence may be the final step that commits the arrested fruitlet to abscission.

While senescence can be induced by stress or physical damage, our results suggest that the degenerative process induced in the seed coat during IFA was triggered by the activation of an age-dependent-like senescence pathway. Competence to undergo fruit senescence or ripening is typically acquired during maturation and is associated with reduced auxin activity together with an increase in ABA (Bower and Cutting, 1988; McAtee *et al.*, 2013; Fenn and Giovannoni, 2021). In addition, ABA derived from maternal organs including the seed coat plays a key role in initiating seed maturation and dormancy (Iwasaki *et al.*, 2022; Kavi Kishor *et al.*, 2022). Further, at a late stage of seed maturation, dormancy is accompanied with a programmed degenerative process in the seed coat, which forms a protective layer around the embryo (Radchuk and Borisjuk, 2014). In our study, the decrease in auxin and increase in ABA in the seed coat and pericarp during fruitlet growth arrest were strikingly similar to the hormonal changes that occur during fruit maturation. Growth arrest was also accompanied by the activation of a dormancy-like program of development as indicated by the upregulation of ABA signaling genes and downregulation of *FT-like* in the seed coat and pericarp. Moreover, the increase in *MFT-like* expression in the embryo and seed coat coincided with the expression of senescence associated genes in the seed coat at late growth arrest. Together, these changes in hormone and gene expression profiles suggest that the different tissues of the fruitlet, including the seed coat, undergo a maturation-like program of development prior to abscission. Further, this maturation-like program of development induced in the seed coat likely functions to commit this maternal organ to senescence.

Hormones that regulate the onset and progression of senescence and ripening include ABA, ET and JA (Fenn and Giovannoni, 2021; Ouyang *et al.*, 2025). In our study, results showed that ABA, ACC (a proxy for ET) and JA-Ile, accumulated in the seed coat at a late stage of growth arrest. In addition, ABA, ET and JA biosynthesis and signaling genes were upregulated predominantly in the seed coat during growth cessation. Interestingly, fruitlets that ceased growth in response to ABA treatment also display a senescence phenotype in the seed coat (Moore-Gordon *et al.*, 1998). In addition, the degeneration of the seed coat and nucellus in fruitlets harvested from excised branches was associated with a burst of ethylene primarily

ACCEPTED MANUSCRIPT

Downloaded from https://academic.oup.com/jxb/advance-article/doi/10.1093/jxb/erag289/8709372 by Qld Dept of Employment, Economic Development & Innovation user on 19 June 2026

derived from the seed coat (Davenport and Manners, 1982). Thus, these findings further implicate ABA and ET signaling in regulating seed coat senescence. Taken together, we speculate that ABA, ACC and JA-Ile collectively function to promote the onset and progression of seed coat senescence in response to low auxin activity during late growth arrest and the shrinkage phase, respectively.

Is the mechanism of IFA conserved across different fruit tree species?

Studies in apple suggest that IFA is initiated in the cortex by ET, which triggers developmental arrest via seed abortion (Botton *et al.*, 2011; Eccher *et al.*, 2015). In contrast, our results suggest that avocado IFA is initiated by hormone signaling originating in the seed coat, which induces seed coat senescence and a seed dormancy-like program, collectively suppressing fruitlet growth. Further, we propose that the activation and progression of seed coat senescence represent the final step in the abscission pathway that triggers the detachment of the fruitlet from the tree. In this context, avocado IFA appears to be mediated by a premature activation of an age-dependent abscission pathway in the seed coat.

The differences between IFA in avocado and apple may be attributed to fundamental differences in fruit structure and development. Avocado is classified botanically as a single-seeded berry in which the fleshy pericarp is derived from the ovary wall (Chanderbali et al., 2013). In contrast, apple is botanically classified as a pome containing multiple seeds, where the edible cortex is primarily derived from the hypanthium of the flower surrounding the ovary (Liu et al., 2020). It is conceivable that the evolutionary and structural differences between a single seeded berry and multi-seeded pome fruit may influence the origin and mechanism of IFA signaling.

In addition to apple and avocado, the hormonal basis of IFA has been studied in other tree crops, including litchi (*Litchi chinensis*) and *Citrus*. Litchi fruit is botanically classified as a single-seeded drupe (Wang et al., 2017), whereas the fruit of *Citrus* is botanically a berry with multiple seeds (Agusti et al., 2025). In litchi, reduced IAA combined with increased ABA and ET in the fruit tissues and/or seed is associated with immature fruit abscission (Kuang *et al.*, 2012; Li *et al.*, 2015; Wang *et al.*, 2024). In *Citrus*, fruitlet abscission is associated with an increase in ABA and ACC in the fruit tissues (Gómez-Cadenas A, 2000). While there appears to be some conservation of hormones implicated in IFA across different fruit tree species, the tissue in which signaling is initiated and the developmental mechanism leading to

ACCEPTED MANUSCRIPT

Downloaded from https://academic.oup.com/jxb/advance-article/doi/10.1093/jxb/erag289/8709372 by Qld Dept of Employment, Economic Development & Innovation user on 19 June 2026

abscission may differ depending on fruit type. Further investigation is required to determine the origin, identity and integration of IFA hormone siganling in diverse fruit systems.

Conclusion

Based on the data presented in this manuscript, a model is presented in which changes in seed coat hormone signaling determines the fate of developing avocado fruitlet (Fig. 10). In this model, IFA is initiated when the seed coat transitions to a senescence program of development. This developmental transition is initiated by a decrease in auxin activity in the seed coat. As auxin levels decline, increased ABA, ACC and JA-Ile collectively act to suppress growth and activate a senescence program of development in the seed coat at late growth arrest. Also, results suggest that an increase of ABA signaling together with a decrease of *FT-like* expression in the seed coat initiates a dormancy-program of development in the seed that promotes *MFT* expression in the embryo at a late stage of growth arrest. Finally, results predict that decreased auxin biosynthesis and activity in the seed coat may ultimately limit auxin transport through the pedicel allowing ET and possibly JA-Ile to activate cell separation in the AZ. All in all, this working model provides a framework for developing new management practices to reduce summer fruit drop in avocado.

Acknowledgements

The authors thank Dr. Ramesh V. Nair, Director of Bioinformatics, Stanford Center for Genomics and Personalized Medicine (SCGPM), Stanford University School of Medicine, 3165 Porter Drive, Palo Alto, CA 94304, USA, for computational and bioinformatics services. This work utilized computing resources provided by the Stanford Genetics Bioinformatics Service Center (GBSC). We are grateful for Dr. Jean Davidson at Cal Polytechnic State University for supporting the bioinformatic analyses. This work was made possible by Neil Delroy and Jasper Farms, as well as Ben Dring and Andrew Harty at Costa Group, for providing the team with access to avocado trees used in our trials. The authors thank Drs Vy Nguyen, Sarah Hake and Ben Trevaskis for critical reading of this manuscript. Lastly, we thank Jacinta Foley and Declan McCauley at Jasper Farms and the Western Australia Department of Primary Industries and Regional Development, respectively, for assistance with field trials. This work is dedicated to the memory of Reuben Hofshi and Samuel Salazar-Garcia.

ACCEPTED MANUSCRIPT

Downloaded from https://academic.oup.com/jxb/advance-article/doi/10.1093/jxb/erag289/8709372 by Qld Dept of Employment, Economic Development & Innovation user on 19 June 2026

Author contributions: A.H. and H.M.S. designed the research. A.H., M.G., P.H. and S.M.M. performed the research; H.M.S, A.H., M.G. C.B. and P.H. analysed the data and H.M.S. and M.G. wrote the manuscript.

Funding information

This work was funded by CSIRO and the Hort Innovation project AV16005 titled "Maximizing yield and reducing seasonal variation", using the avocado research and development levy.

Conflict of interest

The authors declare no conflict of interest.

Data availability:

The raw RNAseq datasets utilized in this study are available at the CSIRO Data Access Portal (https://data.csiro.au).

ACCEPTED MANUSCRIPT

Downloaded from https://academic.oup.com/jxb/advance-article/doi/10.1093/jxb/erag289/8709372 by Qld Dept of Employment, Economic Development & Innovation user on 19 June 2026

References

Adato I, Gazit S. 1977. Role of Ethylene in Avocado Fruit Development and Ripening. Journal of Experimental Botany **28**, 636–643.

Agusti M, Reig C, Martínez-Fuentes A, Mesejo C. 2026. Advances in *Citrus* fruit set and development: A review. Horticulturae **12**, 18.

Altschup SF, Gish W, Miller W, Myers EW, Lipman DJ. 1990. Basic local alignment search tool. Journal of Molecular Biology **215,** 403-410.

Andrews S. 2010. FASTQC: a quality control tool for high throughput sequence data. Babraham Bioinformatics.

Besseau S, Li J, Palva ET. 2012. WRKY54 and WRKY70 co-operate as negative regulators of leaf senescence in *Arabidopsis thaliana*. Journal of Experimental Botany **63**, 2667–2679.

Böttcher C, Keyzers RA, Boss PK, Davies C. 2010. Sequestration of auxin by the indole-3-acetic acid-amido synthetase GH3-1 in grape berry (*Vitis vinifera* L.) and the proposed role of auxin conjugation during ripening. Journal of Experimental Botany **61**, 3615–3625.

Botton A, Eccher G, Forcato C, *et al.* 2011. Signaling pathways mediating the induction of apple fruitlet abscission. Plant Physiology **155**, 185–208.

Botton A, Ruperti B. 2019. The yes and no of the ethylene involvement in abscission. Plants **8**, 187.

Bower JP, Cutting JG. 1988. Avocado fruit development and ripening physiology. Horticulture Reviews **10**, 229–271.

Chanderbali AS, Soltis DE, Soltis PS, Wolstenholme BN. 2013. Taxonomy and botany. In: Schaffer B, Wolstenholme NB, Whiley AW, eds. The Avocado: botany, production and uses. Wallingford: CABI, 31-50.

Chen K, Li GJ, Bressan RA, Song CP, Zhu JK, Zhao Y. 2020. Abscisic acid dynamics, signaling, and functions in plants. Journal of Integrative Plant Biology **62**, 25–54.

Chen GH, Liu CP, Chen SCG, Wang LC. 2012. Role of ARABIDOPSIS A-FIFTEEN in regulating leaf senescence involves response to reactive oxygen species and is dependent on ETHYLENE INSENSITIVE2. Journal of Experimental Botany **63**, 275–292.

Chen M, MacGregor DR, Dave A, Florance H, Moore K, Paszkiewicz K, Smirnoff N, Graham IA, Penfield S. 2014. Maternal temperature history activates Flowering Locus T in fruits to control progeny dormancy according to time of year. Proceedings of the National Academy of Sciences, USA **111**, 18787–18792.

ACCEPTED MANUSCRIPT

Downloaded from https://academic.oup.com/jxb/advance-article/doi/10.1093/jxb/erag289/8709372 by Qld Dept of Employment, Economic Development & Innovation user on 19 June 2026

Clayton-Cuch D, Yu L, Shirley N, Bradley D, Bulone V, Böttcher C. 2021. Auxin treatment enhances anthocyanin production in the non-climacteric sweet cherry (*Prunus avium* l.). International Journal of Molecular Sciences **22**, 10760.

Davenport TL, Manners MM. 1982. Nucellar Senescence and Ethylene Production as they Relate to Avocado Fruitlet Abscission 1. Journal of Experimental Botany **33**, 815–825.

Dobin A, Davis CA, Schlesinger F, Drenkow J, Zaleski C, Jha S, Batut P, Chaisson M, Gingeras TR. 2013. STAR: Ultrafast universal RNA-seq aligner. Bioinformatics **29**, 15–21.

Dong Z, Xiao Y, Govindarajulu R, Feil R, Siddoway ML, Nielsen T, Lunn JE, Hawkins J, Whipple C, Chuck G. 2019. The regulatory landscape of a core maize domestication module controlling bud dormancy and growth repression. Nature Communications **10**, 3810.

Dubois M, Van den Broeck L, Inzé D. 2018. The Pivotal Role of Ethylene in Plant Growth. Trends in Plant Science **23**, 311–323.

Eccher G, Begheldo M, Boschetti A, Ruperti B, Botton A. 2015. Roles of ethylene production and ethylene receptor expression in regulating apple fruitlet abscission. Plant Physiology **169**, 125–137.

Ellis CM, Nagpal P, Young JC, Hagen G, Guilfoyle TJ, Reed JW. 2005. AUXIN RESPONSE FACTOR1 and AUXIN RESPONSE FACTOR2 regulate senescence and floral organ abscission in *Arabidopsis thaliana*. Development **132**, 4563–4574.

Fenn MA, Giovannoni JJ. 2021. Phytohormones in fruit development and maturation. Plant Journal **105**, 446–458.

Figueiredo DD, Köhler C. 2018. Auxin: a molecular trigger of seed development. Genes and Development **32**, 479–490.

Fonseca S, Chini A, Hamberg M, Adie B, Porzel A, Kramell R, Miersch O, Wasternack C, Solano R. 2009. (+)-7-iso-Jasmonoyl-L-isoleucine is the endogenous bioactive jasmonate. Nature Chemical Biology **5**, 344–350.

Footitt S, Ölçer-Footitt H, Hambidge AJ, Finch-Savage WE. 2017. A laboratory simulation of *Arabidopsis* seed dormancy cycling provides new insight into its regulation by clock genes and the dormancy-related genes DOG1, MFT, CIPK23 and PHYA. Plant Cell and Environment **40**, 1474–1486.

Garner LC, Lovatt CJ. 2016. Physiological factors affecting flower and fruit abscission of 'Hass' avocado. Scientia Horticulturae **199**, 32–40.

Gómez-Cadenas A, Mehouachi J, Tadeo FR, Primo-Millo E, Talon M. 2000. Hormonal regulation of fruitlet abscission induced by carbohydrate shortage in citrus. Planta **210**, 636–643.

ACCEPTED MANUSCRIPT

Downloaded from https://academic.oup.com/jxb/advance-article/doi/10.1093/jxb/erag289/8709372 by Qld Dept of Employment, Economic Development & Innovation user on 19 June 2026

Gonzalez-Grandio E, Pajoro A, Franco-Zorrilla JM, Tarancon C, Immink RGH, Cubas P. 2017. Abscisic acid signaling is controlled by a BRANCHED1/HD-ZIP cascade in *Arabidopsis* axillary buds. Proceedings of the National Academy of Sciences, USA **114**, E245–E254.

Greene DW, Lakso AN, Robinson TL, Schwallier P. 2013. Development of a Fruitlet Growth Model to Predict Thinner Response on Apples. HORTSCIENCE **48**, 584–587.

Guo Q, Major IT, Howe GA. 2018. Resolution of growth–defense conflict: mechanistic insights from jasmonate signaling. Current Opinion in Plant Biology **44**, 72–81.

Hou K, Wu W, Gan SS. 2013. SAUR36, a SMALL AUXIN UP RNA gene, is involved in the promotion of leaf senescence in *Arabidopsis*. Plant Physiology **161**, 1002–1009.

Huang H, Liu B, Liu L, Song S. 2017. Jasmonate action in plant growth and development. Journal of Experimental Botany **68**, 1349–1359.

Iwasaki M, Penfield S, Lopez-Molina L. 2022. Parental and Environmental Control of Seed Dormancy in *Arabidopsis thaliana*. Annual Review of Plant Biology 2022 **73**, 2022.

Kavi Kishor PB, Tiozon RN, Fernie AR, Sreenivasulu N. 2022. Abscisic acid and its role in the modulation of plant growth, development, and yield stability. Trends in Plant Science **27**, 1283–1295.

Krueger F, James F, Ewels P, Afyounian E, Schuster-Boeckler B. 2021. TrimGalore. FelixKrueger/TrimGalore.

Kuang JF, Wu JY, Zhong HY, Li CQ, Chen JY, Lu WJ, Li JG. 2012. Carbohydrate stress affecting fruitlet abscission and expression of genes related to auxin signal transduction pathway in litchi. International Journal of Molecular Sciences **13**, 16084–16103.

Kumar R, Khurana A, Sharma AK. 2014. Role of plant hormones and their interplay in development and ripening of fleshy fruits. Journal of Experimental Botany **65**, 4561–4575.

Kushiro T, Okamoto M, Nakabayashi K, Yamagishi K, Kitamura S, Asami T, Hirai N, Koshiba T, Kamiya Y, Nambara E. 2004. The *Arabidopsis* cytochrome P450 CYP707A encodes ABA 8′-hydroxylases: Key enzymes in ABA catabolism. EMBO Journal **23**, 1647–1656.

Li C, Wang Y, Huang X, Li J, Wang H, Li J. 2015. An improved fruit transcriptome and the identification of the candidate genes involved in fruit abscission induced by carbohydrate stress in *litchi*. Frontiers in Plant Science **6**, 439.

Livak KJ, Schmittgen TD. 2001. Analysis of relative gene expression data using real-time quantitative PCR and the 2-ΔΔCT method. Methods **25**, 402–408.

Liu Z, Ma H, Jung S, Main D, Guo L. 2020. Developmental mechanisms of fleshy fruit diversity in *Rosaceae*. Annual Review of Plant Biology **71**, 547-573.

ACCEPTED MANUSCRIPT

Downloaded from https://academic.oup.com/jxb/advance-article/doi/10.1093/jxb/erag289/8709372 by Qld Dept of Employment, Economic Development & Innovation user on 19 June 2026

Love MI, Huber W, Anders S. 2014. Moderated estimation of fold change and dispersion for RNA-seq data with DESeq2. Genome Biology **15**, 550.

Mashiguchi K, Tanaka K, Sakai T, *et al.* 2011. The main auxin biosynthesis pathway in Arabidopsis. Proceedings of the National Academy of Sciences, USA **108**, 18512–18517.

McAtee P, Karim S, Schaffer R, David K. 2013. A dynamic interplay between phytohormones is required for fruit development, maturation, and ripening. Frontiers in Plant Science **4**, 79.

Moore-Gordon CS, Cowan KA, Bertling I, Botha EJ, Cross RH. 1998. Symplastic solute transport and avocado fruit development: A decline in cytokinin/ABA ratio is related to appearance of the Hass small fruit variant. Plant Cell Physiology **39**, 1027–1038.

Morris K, Mackerness SAH, Page T, Fred John C, Murphy AM, Carr JP, Buchanan-Wollaston V. 2000. Salicylic acid has a role in regulating gene expression during leaf senescence. Plant Journal **23**, 677–685.

Mueller-Roeber B, Balazadeh S. 2014. Auxin and Its Role in Plant Senescence. Journal of Plant Growth Regulation **33**, 21–33.

Nakamura S, Abe F, Kawahigashi H, *et al.* 2011. A wheat homolog of MOTHER of FT and TFL1 acts in the regulation of germination. Plant Cell **23**, 3215–3129.

Noh Y-S, Amasino RM. 1999. Identification of a promoter region responsible for the senescence-specific expression of SAG12. Plant Molecular Biology **41**, 181–194.

Ouyang J, He B, Zeng Y, Zhai C, Li Y, Li J, Guan P, Jia W. 2025. The triggering mechanism for predominant hormonal signal production in fleshy fruit ripening. Molecular Horticulture **5**.

Patharkar OR, Walker JC. 2019. Connections between abscission, dehiscence, pathogen defense, drought tolerance, and senescence. Plant Science **284**, 25–29.

Pattyn J, Vaughan-Hirsch J, Van de Poel B. 2021. The regulation of ethylene biosynthesis: a complex multilevel control circuitry. New Phytologist **229,** 770-782.

Pautot V, Crick J, Hepworth SR. 2025. Abscission zones: cellular interfaces for the programmed separation of organs. Annals of Botany **136**, 29–48.

Pérez-Amador MA, Abler ML, De Rocher EJ, Thompson DM, Van Hoof A, Lebrasseur ND, Lers A, Green PJ. 2000. Identification of BFN1, a Bifunctional Nuclease Induced during Leaf and Stem Senescence in Arabidopsis 1. Plant Physiology **122**, 169–179.

Putri GH, Anders S, Pyl PT, Pimanda JE, Zanini F. 2022. Analysing high-throughput sequencing data in Python with HTSeq 2.0. Bioinformatics **38**, 2943–2945.

Radchuk V, Borisjuk L. 2014. Physical, metabolic and developmental functions of the seed coat. Frontiers in Plant Science **5**.

ACCEPTED MANUSCRIPT

Downloaded from https://academic.oup.com/jxb/advance-article/doi/10.1093/jxb/erag289/8709372 by Qld Dept of Employment, Economic Development & Innovation user on 19 June 2026

Rendón-Anaya M, Ibarra-Laclette E, Méndez-Bravo A, *et al.* 2019. The avocado genome informs deep angiosperm phylogeny, highlights introgressive hybridization, and reveals pathogen-influenced gene space adaptation. Proceedings of the National Academy of Sciences, USA **116**, 17081–17089.

Robert HS. 2019. Molecular communication for coordinated seed and fruit development: What can we learn from auxin and sugars? International Journal of Molecular Sciences **20**, 936.

Robert HS, Park C, Gutièrrez CL, *et al.* 2018. Maternal auxin supply contributes to early embryo patterning in Arabidopsis. Nature Plants **4**, 548–553.

Sadka A, Walker CH, Haim D, Bennett T. 2023. Just enough fruit: understanding feedback mechanisms during sexual reproductive development. Journal of Experimental Botany **74**, 2448–2461.

Saito S, Hirai N, Matsumoto C, Ohigashi H, Ohta D, Sakata K, Mizutani M. 2004. Arabidopsis CYP707As encode (+)-abscisic acid 8′-hydroxylase, a key enzyme in the oxidative catabolism of abscisic acid. Plant Physiology **134**, 1439–1449.

Salazar-Garcia S, Garner LC, Lovatt CJ. 2013. Reproductive biology. In: Schaffer B, Wolstenholme NB, Whiley AW, eds. The Avocado: botany, production and uses. Wallingford: CABI, 118–167.

Sawicki M, Aït Barka E, Clément C, Vaillant-Gaveau N, Jacquard C. 2015. Cross-talk between environmental stresses and plant metabolism during reproductive organ abscission. Journal of Experimental Botany **66**, 1707–1719.

Schindelin J, Arganda-Carreras I, Frise E, *et al.* 2012. Fiji: An open-source platform for biological-image analysis. Nature Methods **9**, 676–682.

Sedgley M. 1980. Anatomical Investigation of Abscised Avocado Flowers and Fruitlets. Annals of Botany **46**, 771–777.

Staswick PE, Tiryaki, I. 2004. The oxylipin signal jasmonic acid is activated by an enzyme that conjugates it to isoleucine in *Arabidopsis*. Plant Cell **16**, 2117-2127.

Staswick PE, Serban B, Rowe M, Tiryaki I, Maldonado MT, Maldonado MC, Suza W. 2005. Characterization of an Arabidopsis enzyme family that conjugates amino acids to indole-3-acetic acid. Plant Cell **17**, 616–627.

Trapnell C, Williams BA, Pertea G, Mortazavi A, Kwan G, Van Baren MJ, Salzberg SL, Wold BJ, Pachter L. 2010. Transcript assembly and quantification by RNA-Seq reveals unannotated transcripts and isoform switching during cell differentiation. Nature Biotechnology **28**, 511–515.

Wang J, Ma W, Wang F, He Z, Ye X, Deng J, Zhao M, Li J. 2024. Signaling pathways mediating the induction of preharvest fruit drop in litchi. Frontiers in Plant Science **15**, 1474657.

ACCEPTED MANUSCRIPT

Downloaded from https://academic.oup.com/jxb/advance-article/doi/10.1093/jxb/erag289/8709372 by Qld Dept of Employment, Economic Development & Innovation user on 19 June 2026

Wang HC, Lai, B. Huang, X. 2017. Litchi fruit set, development and maturation. In: Kumar M, Kumar V, Prasad R, Varma A, eds. The lychee biotechnology. Singapore, Springer Nature, 1-30.

Ward D, Marini RP. 1999. Growth and Development of Young Apple Fruits Following Applications of Ethephon Plus Carbaryl for Thinning. HORTSCIENCE **34**, 1057–1059.

Weng JK, Ye M, Li B, Noel JP. 2016. Co-evolution of Hormone Metabolism and Signaling Networks Expands Plant Adaptive Plasticity. Cell **166**, 881–893.

Won C, Shen X, Mashiguchi K, Zheng Z, Dai X, Cheng Y, Kasahara H, Kamiya Y, Chory J, Zhao Y. 2011. Conversion of tryptophan to indole-3-acetic acid by tryptophan aminotransferases of Arabidopsis and YUCCAs in *Arabidopsis*. Proceedings of the National Academy of Sciences, USA **108**, 18518–18523.

Wu A, Allu AD, Garapati P, *et al.* 2012. JUNGBRUNNEN1, a reactive oxygen species-responsive NAC transcription factor, regulates longevity in *Arabidopsis*. Plant Cell **24**, 482–506.

Xi W, Liu C, Hou X, Yu H. 2010. MOTHER OF FT and TFL1 regulates seed germination through a negative feedback loop modulating ABA signaling in *Arabidopsis*. Plant Cell **22**, 1733–1748.

ACCEPTED MANUSCRIPT

Downloaded from https://academic.oup.com/jxb/advance-article/doi/10.1093/jxb/erag289/8709372 by Qld Dept of Employment, Economic Development & Innovation user on 19 June 2026

Alternative figure legends

Fig. 1. Experimental design for capturing persisting and abscising fruitlets undergoing growth arrest. (A) In the natural abscission trial, the diameter of 192 fruitlets was monitored at regular intervals across six trees. Six normal growing (NA-Normal) and six arresting (NA-Arresting) fruitlets with mean growth rates of 0.49 and 0.03 mm/day, respectively, were harvested. Fruitlets were subsequently dissected into seed coat, pericarp and embryo and used for RNA-sequencing and hormone profiling. (B) In the defoliation-induced abscission trial, the growth rate of 100 fruitlets across three defoliated trees and 80 fruitlets across three untreated control trees were evaluated at regular intervals. Six-days after defoliation, five normal growing (DEF-Early) and five arresting (DEF-Late) fruitlets with mean growth rates equal to 0.60 and 0.10 mm/day, respectively, were harvested from the defoliated trees. On the same day, normal growing fruitlets harvested from untreated control trees (UtC-Control) with a mean growth rate of 0.65 mm/day were also harvested. The sampled UtC-Control, DEF-Early and DEF-Late fruitlets were dissected into seed coat, pericarp and embryo for RNA-sequencing. Green and orange circles represent normal growing and arresting fruitlets, respectively. Circles with light green or light orange outlines indicate the trees from which normal-growing (NA-Normal, UtC-Control and DEF-Early) or arresting (NA-Arresting and DEF-Late) fruitlets were harvested.

ALT TEXT: Schematic overview of two experimental designs used to study fruitlet abscission. A is an illustration of the natural abscission trial in which fruitlet growth trajectories were evaluated and used to identify normal-growing (NA-Normal) and arresting fruitlets (NA-Arresting). B is an illustration of the defoliation-induced abscission trial in which fruitlet growth rates were evaluated and used to identify normal-growing fruitlets from untreated control trees (UtC-Normal) and early (DEF-Early) and late (DEG-Late) arresting fruitlets from defoliated trees. Fruitlets are colour-coded by growth status and sampling origin. All sampled fruitlets were dissected into seed coat, pericarp, and embryo for downstream analyses.

ACCEPTED MANUSCRIPT

Downloaded from https://academic.oup.com/jxb/advance-article/doi/10.1093/jxb/erag289/8709372 by Qld Dept of Employment, Economic Development & Innovation user on 19 June 2026

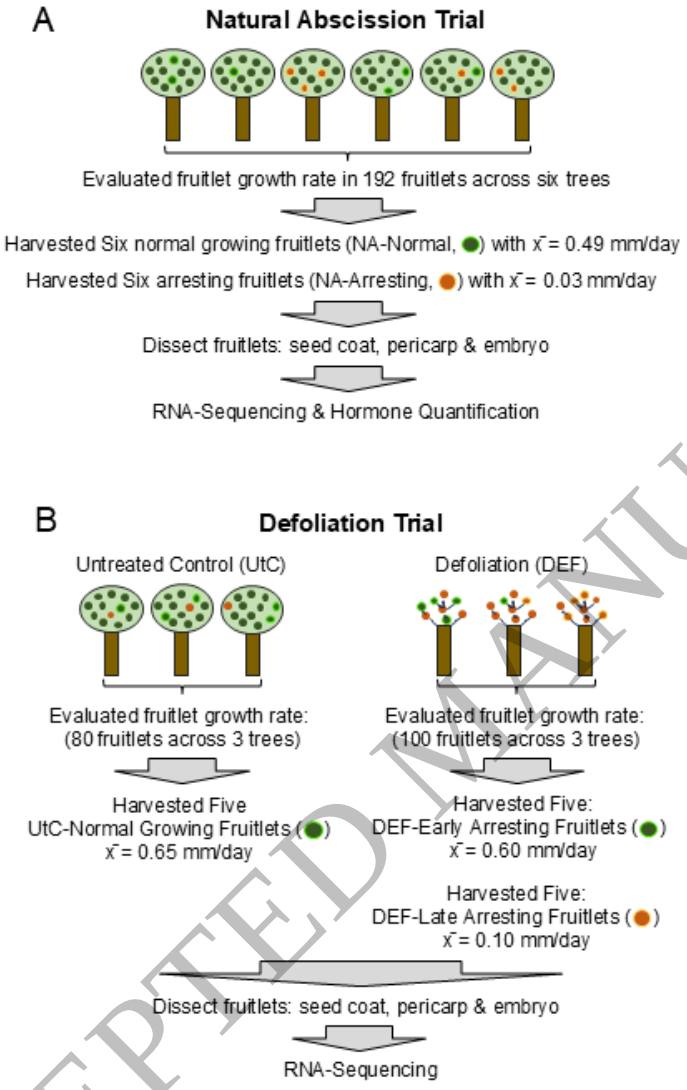

ACCEPTED MANUSCRIPT

Downloaded from https://academic.oup.com/jxb/advance-article/doi/10.1093/jxb/erag289/8709372 by Qld Dept of Employment, Economic Development & Innovation user on 19 June 2026

Fig. 2. Fruit growth arrest is an early event in the IFA pathway. (A) Fruitlet growth was assessed using digital dendrometers from 73 to 129 days after full bloom (DAFB; *n*=34, fruitlets). (B) Mean growth rate (mm/day) of persisting fruitlets was determined from 73 to 129 DAFB (*n*=34, fruitlets). (C) Cumulative and (D) daily fruitlet percent abscission during the growing phase of development (*n*=5, tree). (E) Mean growth rate of fruitlets that abscised was collated and plotted against days to fruit drop (*n*=22), where abscission occurred on day zero. Dots represent the mean and shaded regions indicate the range of values.

ALT TEXT: Graphs labelled A to E. A is a graph that displays a change in the diameter (mm) of developing fruitlets over time (day). B is a graph showing the growth rate (mm/day) of developing fruitlets over time. C is a graph that displays percent fruitlet abscission over time (day). D is a graph showing the percent of daily fruitlet abscission overtime (day). E is a graph that displays the change in the rate of fruitlet growth (mm/day) prior to fruitlet abscission.

ACCEPTED MANUSCRIPT

Downloaded from https://academic.oup.com/jxb/advance-article/doi/10.1093/jxb/erag289/8709372 by Qld Dept of Employment, Economic Development & Innovation user on 19 June 2026

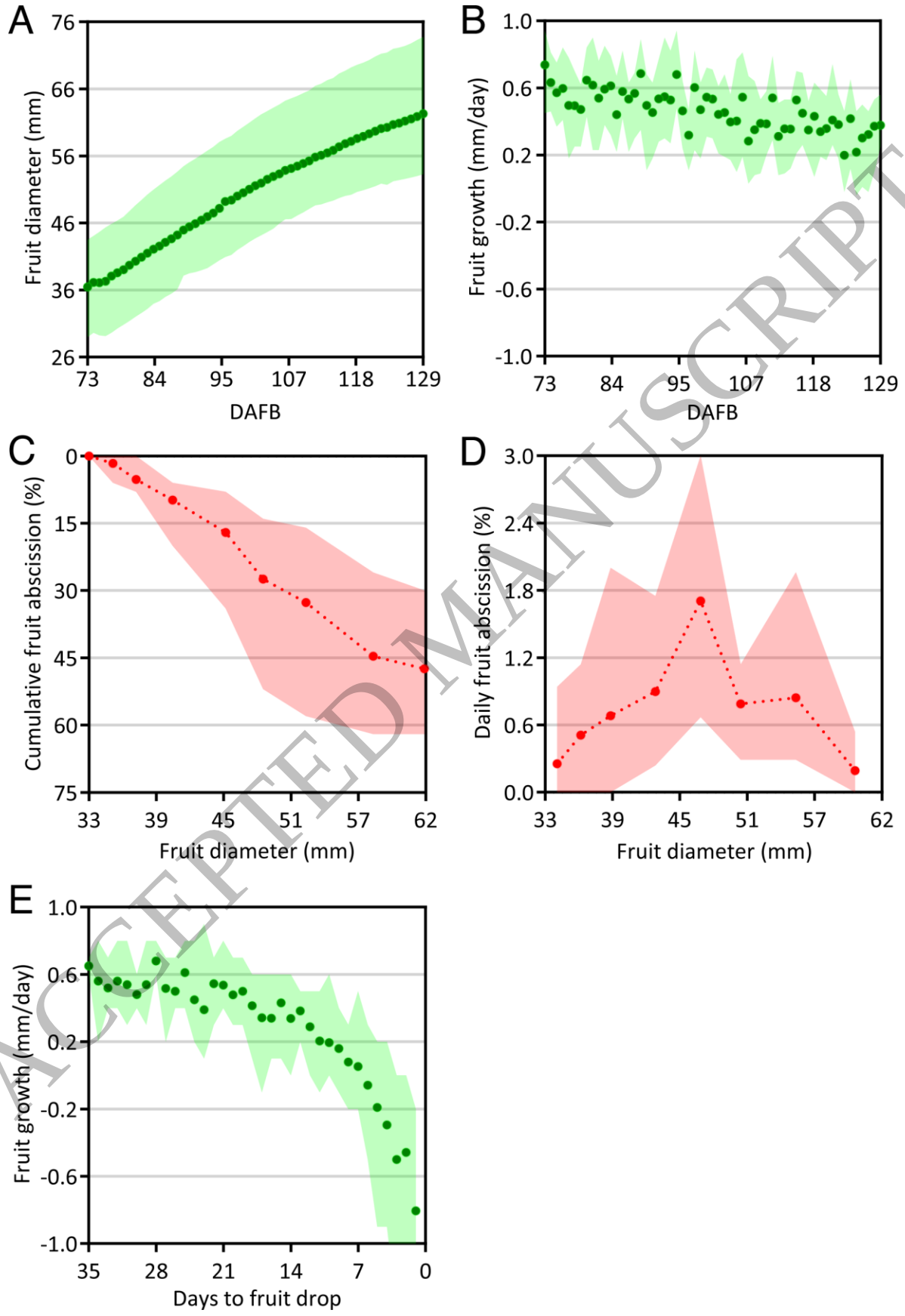

ACCEPTED MANUSCRIPT

Downloaded from https://academic.oup.com/jxb/advance-article/doi/10.1093/jxb/erag289/8709372 by Qld Dept of Employment, Economic Development & Innovation user on 19 June 2026

Fig. 3. Seed coat and pericarp transcriptomes are highly responsive to the growth arrest signal(s). (A) Principal component analysis (PCA) of seed coat, pericarp and embryo transcriptomes from normal-growing (NA-Normal) and arresting (NA-Arresting) fruitlets under natural conditions (*n*=5 fruitlets per condition). PCA also includes transcriptomes from seed coat, pericarp and embryo derived from fruitlets sampled from defoliated (DEF-Early and DEF-Late) and untreated control (UtC-Normal) trees (*n*=5 fruitlets per condition). (B) DEGs associated with natural growth arrest (NGA) were identified by comparing NA-Normal and NA-Arresting transcriptomes for each tissue. (C, D) DEGs associated with early and late growth arrest were identified by comparing UtC-Normal transcriptomes with DEF-Early (DEGA) and DEF-Late (DGA) transcriptomes, respectively. (E-G) Venn diagrams show shared and unique DEGs in the (E) seed coat, (F) pericarp and (G) embryo for the NGA, DEGA, and DGA comparisons.

ALT TEXT: Multi-panel figure showing the responsiveness of the seed coat, pericarp and embryo transcriptomes to growth arrest. A is a graph that displays principal component analysis for the variation in the seed coat, pericarp and embryo transcriptomes in response to growth arrest. B to D are illustrations showing how differentially expressed genes were identified in response to natural (NGA) and defoliated (DEGA and DGA) induced growth arrest for the seed coat, pericarp and embryo. Venn diagrams show shared and unique transcriptional responses in the (E) seed coat and (F) pericarp compared to (G) embryo.

ACCEPTED MANUSCRIPT

Downloaded from https://academic.oup.com/jxb/advance-article/doi/10.1093/jxb/erag289/8709372 by Qld Dept of Employment, Economic Development & Innovation user on 19 June 2026

OFFICIAL

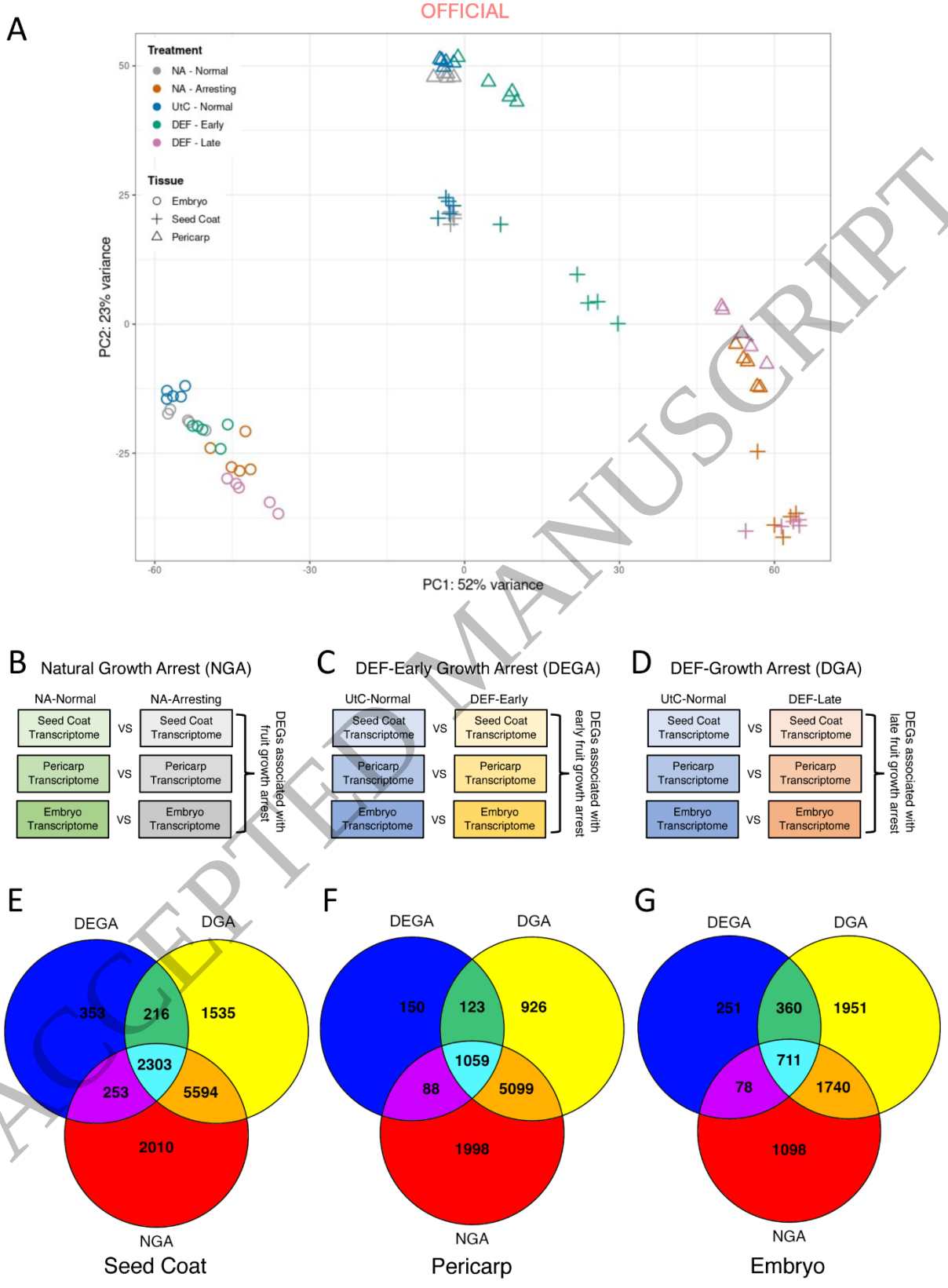

ACCEPTED MANUSCRIPT

Downloaded from https://academic.oup.com/jxb/advance-article/doi/10.1093/jxb/erag289/8709372 by Qld Dept of Employment, Economic Development & Innovation user on 19 June 2026

1

Fig. 4. Regulation of free auxin levels in response to fruitlet growth arrest. (A) Free indole-3-acetic acid (IAA; black box) is regulated by the TAA1/YUC biosynthesis pathway and GH3, which conjugates IAA with aspartic acid (Asp) or other amino acids. Differential expression of (B) IAA biosynthesis (*YUCCA*) and (C) conjugation (*GH3*) genes between normal growing and arresting fruit tissues under natural conditions (NGA, n=5). Temporal expression of (B) *YUCCA* and (C) *GH3* genes in the seed coat, pericarp and embryo during early (DEGA) and late (DGA) stages of growth arrest in response to defoliation (n=5). Heatmaps display $\log_2$ fold change of expression using a colour gradient. Genes with a log2 fold change ≤ 1 were assigned a zero value. (D) Free IAA and (E) IAA-Asp in the seed coat, pericarp and embryo in NA-Normal and NA-Arresting fruitlets. IAA and IAA-Asp levels are shown as nmol/g of fresh weight (FW). Six biological replicates were used for all samples except the arresting seed coat (SC), which was derived from five biological replicates. Box plots shows the interquartile range (box) with maximum and minimum values indicated by whiskers. The mean and median are represented by a plus sign and a horizontal line, respectively, within the box. Asterisks indicate statistically significant differences using the Student's t-test (p≤0.01).

ALT TEXT: Multi-panel figure illustrating alterations in auxin (IAA) homeostasis during fruitlet growth arrest. A is an illustration of a major IAA biosynthesis and conjugation pathway in plants. B and C are heatmaps displaying gene expression changes for *YUC-like* and *GH3-like* in response to natural (NGA) and defoliated (DEGA and DGA) induced growth arrest. The colour in the heatmap illustrates whether a gene is upregulated (yellow to dark red) or downregulated (blue green to dark blue). D and E are box plots showing the differences in free IAA and conjugated IAA-Asp levels between normal-growing (NA-Normal; black) and arresting fruitlets (NA-Arresting; red) at a late stage of growth arrest.

ACCEPTED MANUSCRIPT

Downloaded from https://academic.oup.com/jxb/advance-article/doi/10.1093/jxb/erag289/8709372 by Qld Dept of Employment, Economic Development & Innovation user on 19 June 2026

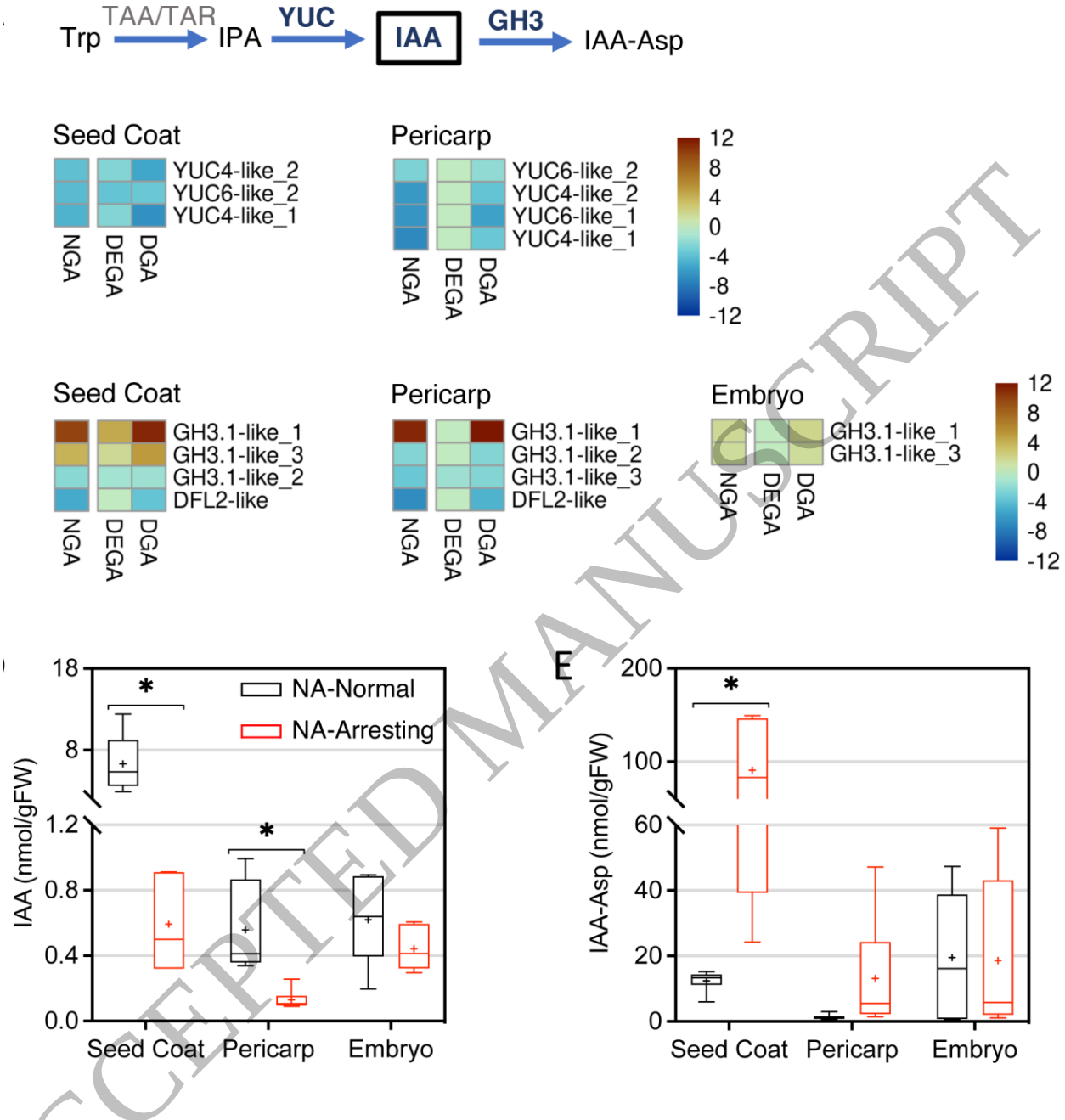

Fig. 5. ABA biosynthesis and catabolism during fruitlet growth arrest. (A) In the ABA biosynthesis pathway, NCED catalyzes the conversion of 9-*cis*-neoxanthin or 9-*cis*-violaxanthin to xanthoxin, while ABA2 converts xanthoxin to abscisic aldehyde. In the last step, abscisic aldehyde is converted to ABA by AAO3. The homeobox-leucine zipper transcription factor, HB40, activates *NCED* gene expression. (B) Differential expression of ABA biosynthesis genes in the seed coat, pericarp and embryo during natural growth arrest (NGA, *n*=5) and during early (DEGA, *n*=5) and late stages (DGA, *n*=5) of defoliated-mediated growth arrest. (C) ABA is metabolised to phaseic acid (PA) and dihydro phaseic acid (DPA) by

ACCEPTED MANUSCRIPT

Downloaded from https://academic.oup.com/jxb/advance-article/doi/10.1093/jxb/erag289/8709372 by Qld Dept of Employment, Economic Development & Innovation user on 19 June 2026

CYP707As and PAR, respectively. (D) Differential expression of *CYP707A* genes in the seed coat, pericarp and embryo during natural growth arrest (NGA, n=5) and during early (DEGA, n=5) and late stages (DGA, n=5) of defoliated-mediated growth arrest. Quantification of (E) ABA, (F) PA and (G) DPA in seed coat (SC), pericarp (PE) and embryo (EM) from NA-Normal and NA-Arresting fruitlets. These hormone metabolites are shown as nmol/g fresh weight (FW). Six biological replicates were used for all samples except the arresting seed coat, which included five biological replicates. (B, D) Heatmaps show the $\log_2$ fold change of expression displayed by a gradient colour scale. Genes with a $\log_2$ fold change $\leq$1, were assigned a zero expression value. (E-G) Box plots show the interquartile range (box) with maximum and minimum values represented by whiskers. The mean and median are represented by a plus sign and horizontal line, respectively, within the box. Asterisks indicate a statistically significant difference according to Student's t-test (*p≤0.05; **p≤0.01).

ALT TEXT: Multi-panel figure illustrating changes in ABA homeostasis during fruitlet growth arrest. A is an illustration of the ABA biosynthesis pathway in plants. Heatmaps displayed in B show changes in the expression of ABA biosynthesis genes during natural (NGA) and defoliated (DEGA and DGA) induced growth arrest. C is an illustration of the ABA catabolism pathway in plants. Heatmaps displayed in D show changes in the expression of *CYP707A-like* in response to natural and defoliated induced growth arrest. The colour in the heatmap displayed in B and D show whether a gene is upregulated (yellow to dark red) or downregulated (blue green to dark blue). E to F are box plots showing the differences in ABA, PA and DPA levels between normal-growing (NA-Normal; black) and arresting fruitlets (NA-Arresting; red) at a late stage of growth arrest.

ACCEPTED MANUSCRIPT

Downloaded from https://academic.oup.com/jxb/advance-article/doi/10.1093/jxb/erag289/8709372 by Qld Dept of Employment, Economic Development & Innovation user on 19 June 2026

OFFICIAL

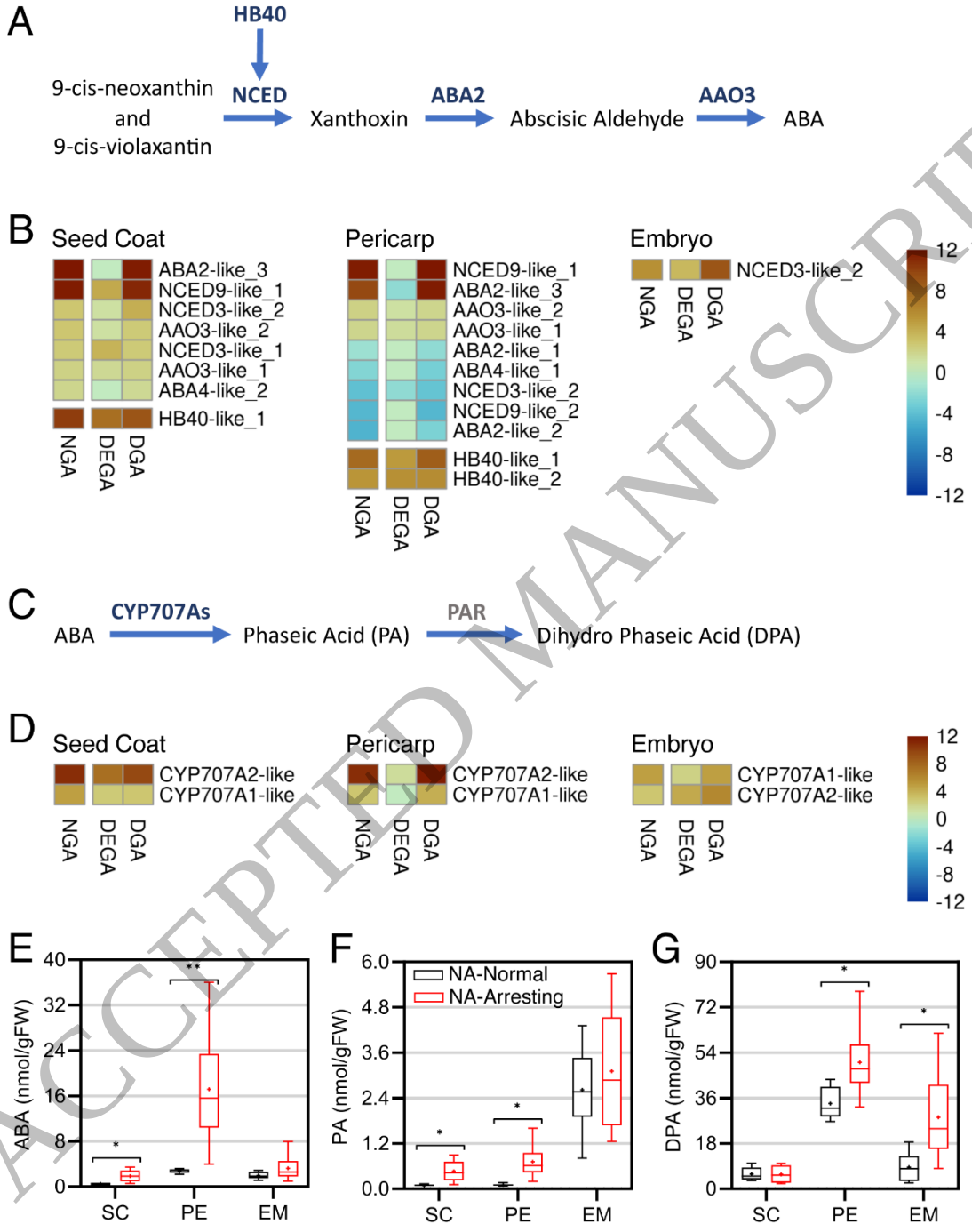

ACCEPTED MANUSCRIPT

Downloaded from https://academic.oup.com/jxb/advance-article/doi/10.1093/jxb/erag289/8709372 by Qld Dept of Employment, Economic Development & Innovation user on 19 June 2026

OFFICIAL

Fig. 6. Accumulation of the ET precursor, ACC, in the seed coat during fruitlet growth arrest. (A) In the ET biosynthesis pathway, ACS and ACO catalyze the conversion of SAM to ACC and ACC to ET, respectively. (B) Differential expression of ET biosynthesis genes in the seed coat, pericarp and embryo during natural growth arrest (NGA, *n*=5) and during early (DEGA, *n*=5) and late stages (DGA, *n*=5) of defoliated-mediated growth arrest. Heatmaps show the $\log_2$ fold change of expression displayed by a gradient colour scale. Genes with a $\log_2$ fold change ≤ 1, were assigned a zero expression value. (C) ACC was quantified in the seed coat, pericarp and embryo in NA-Normal and NA-Arresting fruits with levels shown by nmol/g of fresh weight (FW). Six biological replicates were used for all samples except the arresting seed coat, which included five biological replicates. Box plots show the interquartile range (box) with maximum and minimum values represented by whiskers. The mean and median are represented by a plus sign and horizontal line, respectively, within the box. Asterisks indicate statistically significant differences according to the Student's t-test (**$p \leq 0.01$; ***$p \leq 0.001$).

ALT TEXT: Multi-panel figure illustrating changes in ACC homeostasis during fruitlet growth arrest. A is an illustration of the ACC/ET biosynthesis pathway in plants. Heatmaps displayed in B show changes in the expression of ACC and ET biosynthesis genes during natural (NGA) and defoliated (DEGA and DGA) induced growth arrest. The colour in the heatmaps displayed in B show whether a gene is upregulated (yellow to dark red) or downregulated (blue green to dark blue). C is a box plot showing the differences in ACC levels between normal-growing (NA-Normal; black) and arresting fruitlets (NA-Arresting; red) at a late stage of growth arrest.

ACCEPTED MANUSCRIPT

Downloaded from https://academic.oup.com/jxb/advance-article/doi/10.1093/jxb/erag289/8709372 by Qld Dept of Employment, Economic Development & Innovation user on 19 June 2026

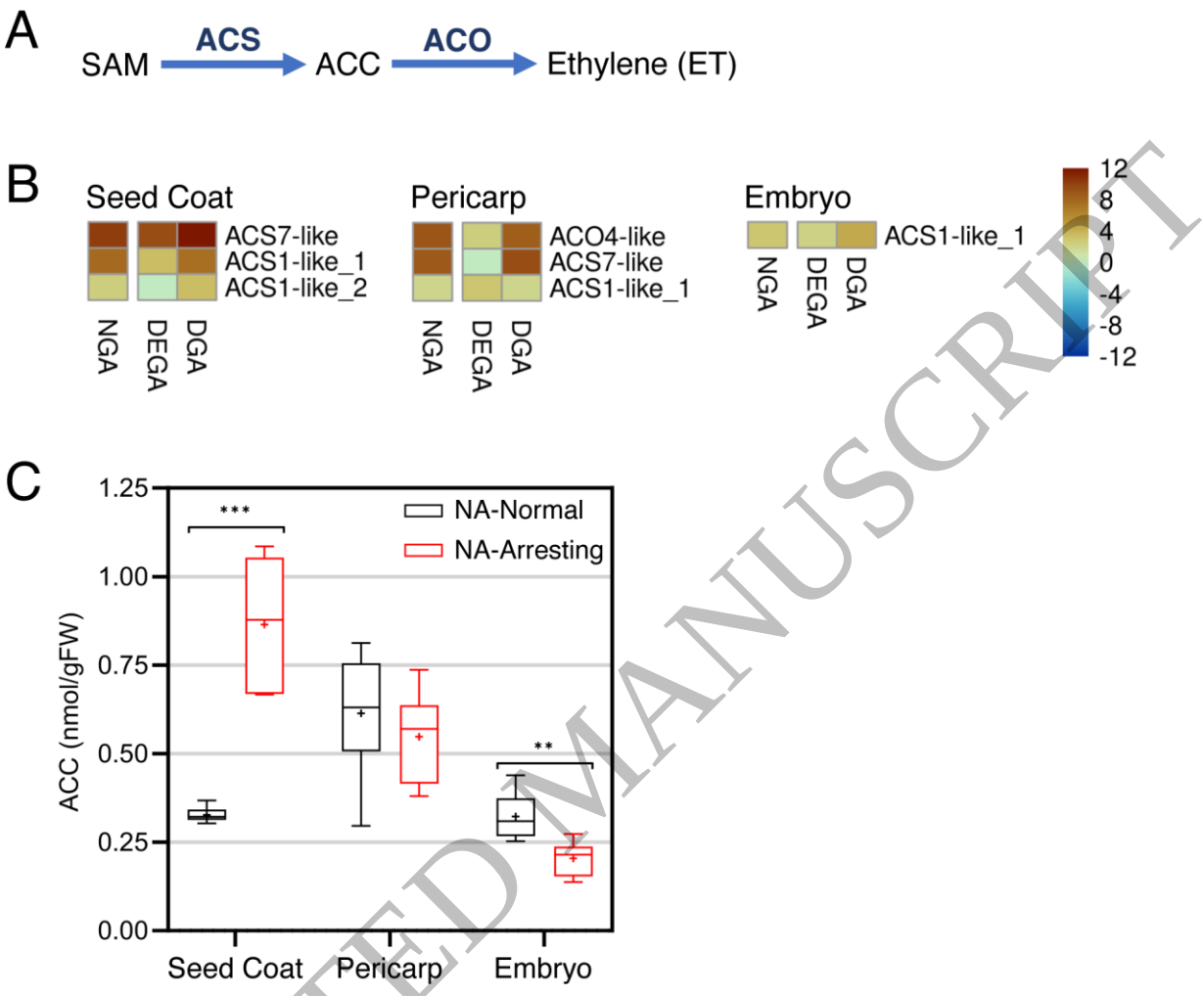

Fig. 7. Jasmonate accumulation in the seed coat during fruitlet growth arrest. (A) In the JA biosynthesis pathway, a-linolenic acid is converted to JA in a multistep process involving LOX, AOS, AOC and OPR3. (B) Differential expression of JA biosynthesis genes in the seed coat, pericarp and embryo during natural growth arrest (NGA, *n*=5) and during early (DEGA, *n*=5) and late stages (DGA, *n*=5) of defoliated-mediated growth arrest. Heatmaps show the $\log_2$ fold change of expression displayed by a gradient colour scale. Genes with a $\log_2$ fold change ≤ 1, were assigned a zero expression value. Quantification of (C) JA and (D) JA-Ile in seed coat, pericarp and embryo of NA-Normal and NA-Arresting fruitlets. Hormone metabolite levels are shown as nmol/g fresh weight (FW). Six biological replicates were used for all samples except the arresting seed coat, which included five biological replicates. Box plots show the interquartile range (box) with maximum and minimum values represented by whiskers. The mean and median are represented by a plus sign and horizontal line,

ACCEPTED MANUSCRIPT

Downloaded from https://academic.oup.com/jxb/advance-article/doi/10.1093/jxb/erag289/8709372 by Qld Dept of Employment, Economic Development & Innovation user on 19 June 2026

respectively, within the box. Asterisks indicate statistically significant differences according to the Student's t-test (*$p \leq 0.05$; **$p \leq 0.01$).

ALT TEXT: Multi-panel figure illustrating changes in JA/JA-Ile homeostasis during fruitlet growth arrest. A is an illustration of the JA/JA-Ile biosynthesis pathway in plants. Heatmaps displayed in B show changes in the expression of JA biosynthesis genes during natural (NGA) and defoliated (DEGA and DGA) induced growth arrest. The colour in the heatmaps displayed in B show whether a gene is upregulated (yellow to dark red) or downregulated (blue green to dark blue). C and D display box plots showing the differences in JA and JA-Ile levels, respectively, between normal-growing (NA-Normal; black) and arresting fruitlets (NA-Arresting; red) at a late stage of growth arrest.

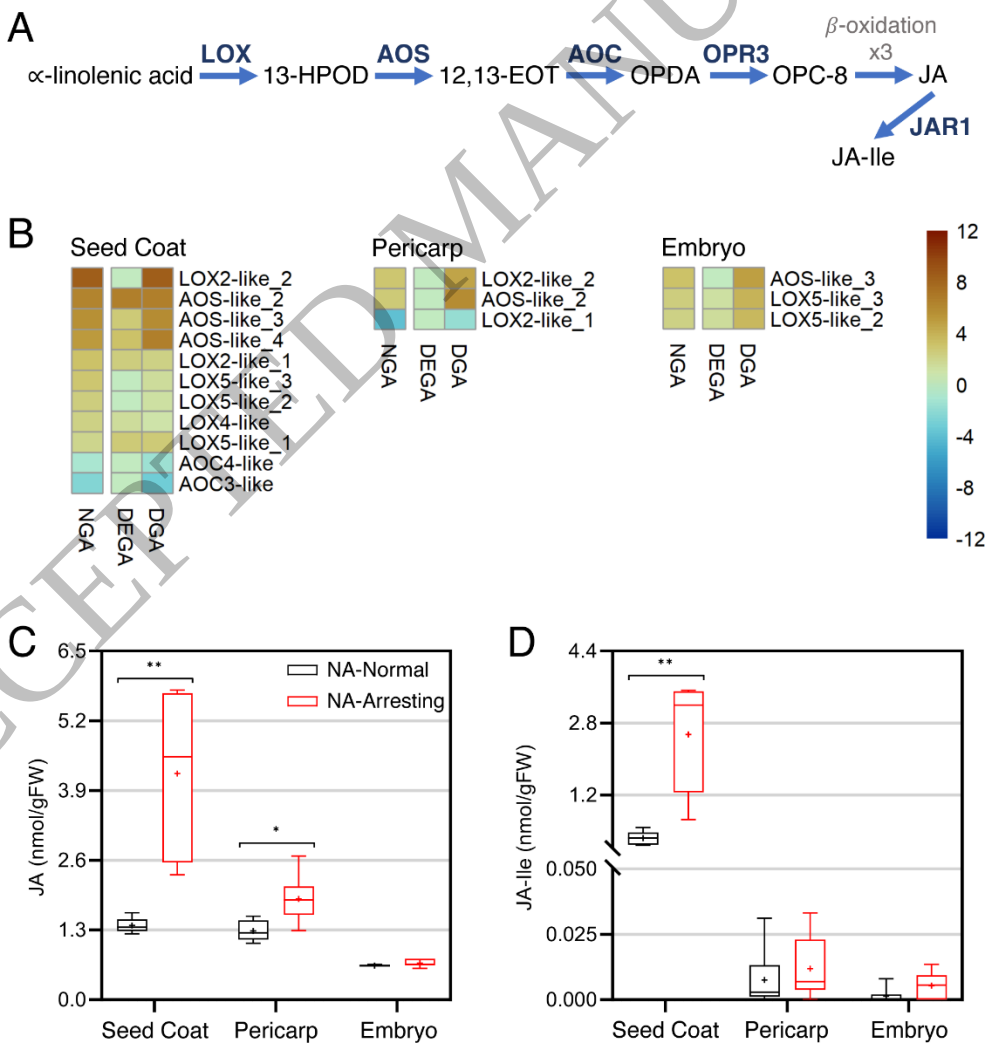

ACCEPTED MANUSCRIPT

Downloaded from https://academic.oup.com/jxb/advance-article/doi/10.1093/jxb/erag289/8709372 by Qld Dept of Employment, Economic Development & Innovation user on 19 June 2026

Fig. 8. Timing of seed coat senescence in the IFA pathway. Representative appearance of the seed coat in (A) normal growing and (B) recently abscised fruitlets. (C) The senescence phenotype was quantified in seed coat images derived from fruitlets exhibiting different growth rates, including arresting, shrinking and recently abscised fruitlets (*n*=127; Fig. S12). The graph shows the mean percentage of senescence-associated pixels per seed coat image for each growth-rate category. Values are means ± standard error of the mean (SEM). Different letters above the bars (a, b or c) indicate statistically significant differences determined by one-way analysis of variance (ANOVA) followed by Tukey's honestly significant difference test (adjusted $p < 0.05$). (D) Differential expression of senescence associated genes in the seed coat during natural growth arrest (NGA, *n*=5) and during early (DEGA, *n*=5) and late stages (DGA, *n*=5) of defoliated-mediated growth arrest. Heatmaps show the $\log_2$ fold change of expression displayed by a gradient colour scale. Genes with a $\log_2$ fold change ≤ 1, were assigned a zero expression value. Brackets in (A) and (B) mark the seed coat (SC), which was visualized by removing of the embryo.

ALT TEXT: Multi-panel figure illustrating the timing of seed coat senescence. Representative image of a seed coat from (A) normal-growing and (B) recently abscised fruitlet. C is a graph that displays quantitative changes in seed coat senescence in growing, arresting and shrinking fruitlets prior to abscission. The heatmaps displayed in B show changes in the expression of senescence associated genes during natural (NGA) and defoliated (DEGA and DGA) induced growth arrest. The colour in the heatmaps displayed in B show whether a gene is upregulated (yellow to dark red) or downregulated (blue green to dark blue).

ACCEPTED MANUSCRIPT

Downloaded from https://academic.oup.com/jxb/advance-article/doi/10.1093/jxb/erag289/8709372 by Qld Dept of Employment, Economic Development & Innovation user on 19 June 2026

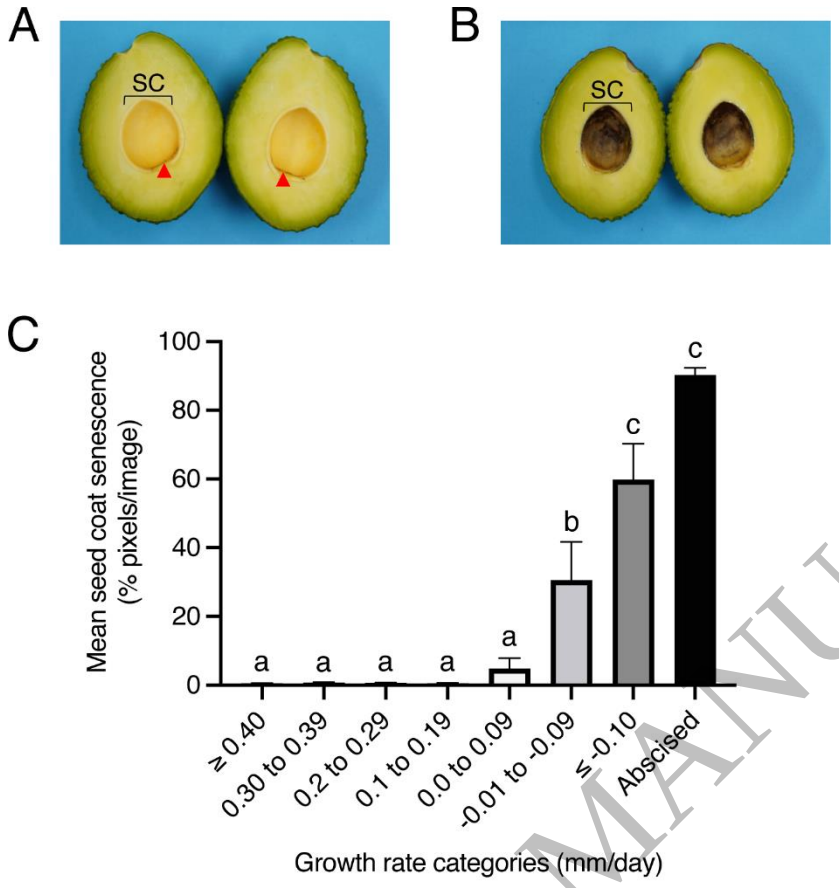

ACCEPTED MANUSCRIPT

Downloaded from https://academic.oup.com/jxb/advance-article/doi/10.1093/jxb/erag289/8709372 by Qld Dept of Employment, Economic Development & Innovation user on 19 June 2026

OFFICIAL

Fig. 9. Differential expression of seed dormancy signaling genes during fruitlet growth arrest. Representative cross-sections of a (A) persisting and (B) recently abscised fruitlet (EM, embryo; red arrow head points to seed coat). (C) Schematic representation of dormancy signaling pathways. (D and E) Differential expression of dormancy signaling genes in the seed coat, pericarp and embryo during natural growth arrest (NGA, *n*=5) and during early (DEGA, *n*=5) and late stages (DGA, *n*=5) of defoliated-mediated growth arrest. Heatmaps show the $\log_2$ fold change of expression displayed by a gradient colour scale. Genes with a $\log_2$ fold change ≤ 1, were assigned a zero expression value.

ALT TEXT: Multi-panel figure illustrating the activation of dormancy-like response during late growth arrest. (A and B) A normal growing and recently abscised fruitlet was cut longitudinally and one half of the fruitlet was imaged to show the appearance of the embryo, as well as pericarp and seed coat. C is an illustration of ABA and FT/MFT siganling pathways that control seed dormancy in plants. The heatmaps displayed in D and E show changes in the expression of dormancy signaling genes during natural (NGA) and defoliated (DEGA and DGA) induced growth arrest. The colour in the heatmaps displayed in B show whether a gene is upregulated (yellow to dark red) or downregulated (blue green to dark blue).

ACCEPTED MANUSCRIPT

Downloaded from https://academic.oup.com/jxb/advance-article/doi/10.1093/jxb/erag289/8709372 by Qld Dept of Employment, Economic Development & Innovation user on 19 June 2026

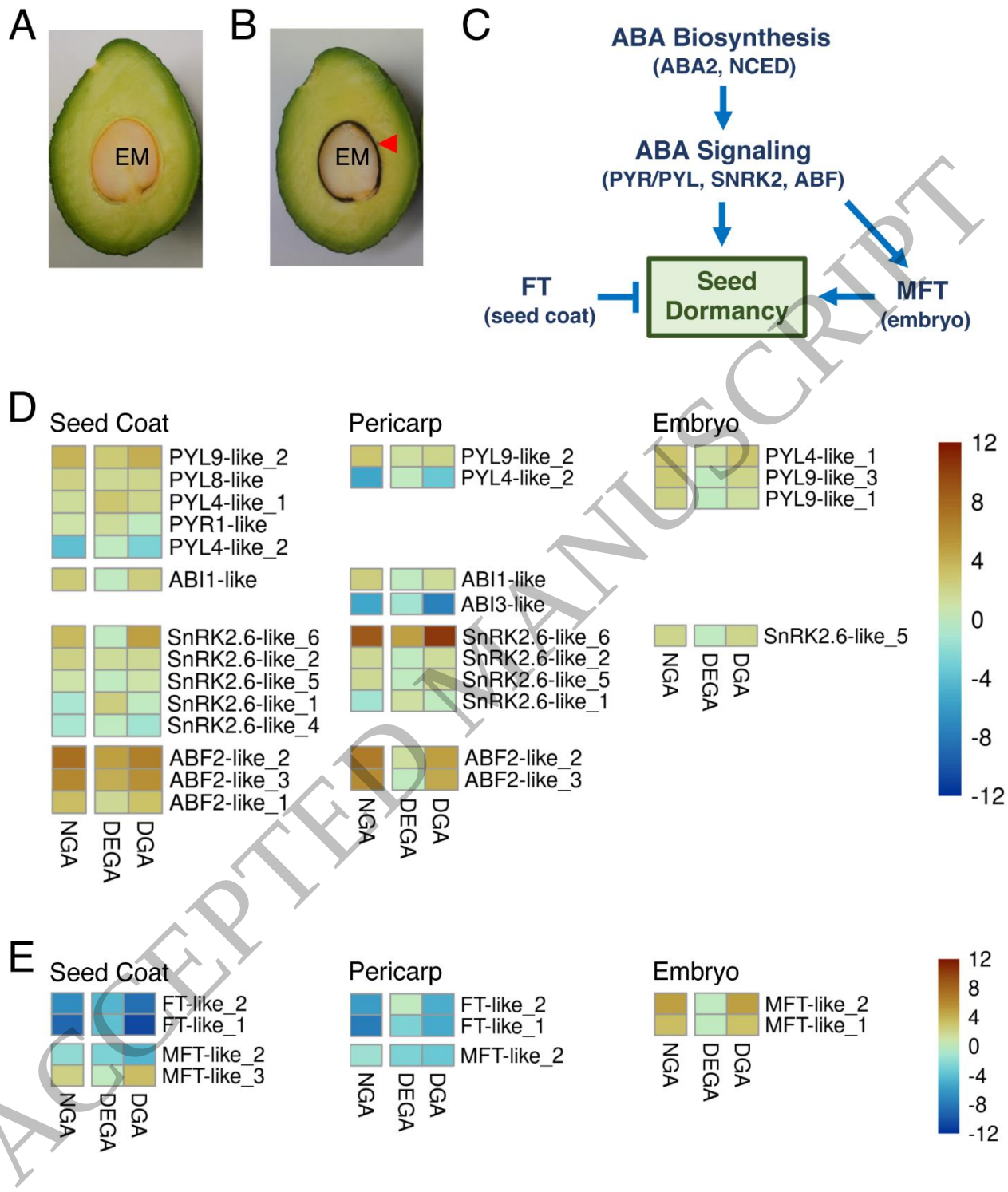

ACCEPTED MANUSCRIPT

Downloaded from https://academic.oup.com/jxb/advance-article/doi/10.1093/jxb/erag289/8709372 by Qld Dept of Employment, Economic Development & Innovation user on 19 June 2026

Fig. 10. Model for the role of the seed coat in avocado fruitlet abscission. In this model, the IFA signaling event is initiated in the seed coat by a decrease in auxin activity, which is transmitted to the pericarp and embryo to induce fruitlet growth arrest. As auxin activity declines, the increase in ABA, ACC and JA-Ile collectively acts to promote a senescence program of development in the seed coat, which suppresses growth and triggers fruitlet abscission. During the transition to seed coat senescence, ABA accumulation in the maternal organs induces seed dormancy.

ALT TEXT: Conceptual model illustrating the role of the seed coat in avocado fruitlet abscission. The model predicts that the abscission signal is initiated the seed coat through reduced auxin activity and transmitted to the pericarp and embryo to induce growth arrest. The decline in auxin is associated with increased ABA, ACC, and JA-Ile, which collectively promotes a senescence program in the seed coat leading to abscission. Increased ABA in the seed coat, as well as the embryo, activates a seed dormancy-like program during late growth arrest.

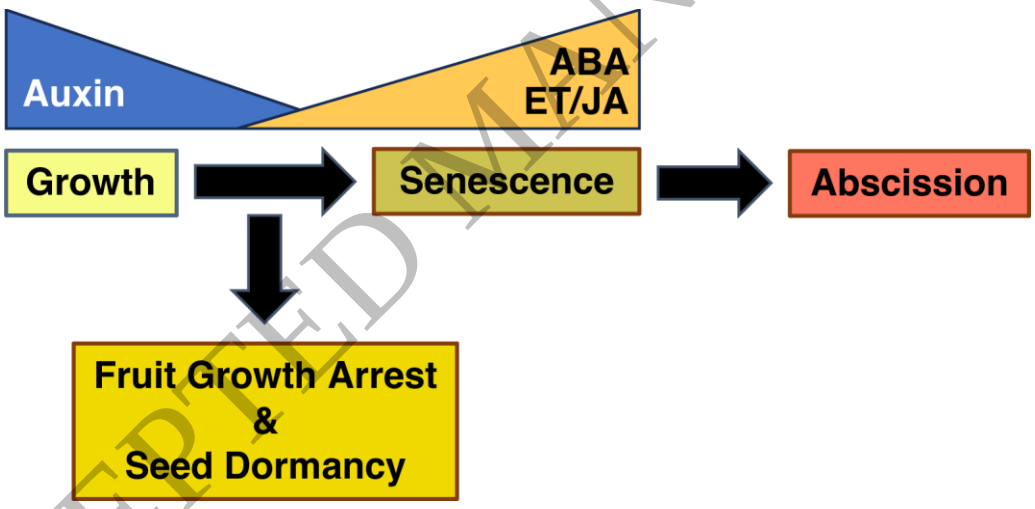

ACCEPTED MANUSCRIPT

Downloaded from https://academic.oup.com/jxb/advance-article/doi/10.1093/jxb/erag289/8709372 by Qld Dept of Employment, Economic Development & Innovation user on 19 June 2026